isvr Institute of Sound and Vibration Research

Vibrational Analysis of a Non-Uniform One-Dimensional Structure Using a Wave Approach

S-K. Lee, B.R. Mace and M.J. Brennan

ISVR Technical Memorandum 918

September 2003

University of Southampton

SCIENTIFIC PUBLICATIONS BY THE ISVR

Technical Reports are published to promote timely dissemination of research results by ISVR personnel. This medium permits more detailed presentation than is usually acceptable for scientific journals. Responsibility for both the content and any opinions expressed rests entirely with the author(s).

Technical Memoranda are produced to enable the early or preliminary release of information by ISVR personnel where such release is deemed to the appropriate. Information contained in these memoranda may be incomplete, or form part of a continuing programme; this should be borne in mind when using or quoting from these documents.

Contract Reports are produced to record the results of scientific work carried out for sponsors, under contract. The ISVR treats these reports as confidential to sponsors and does not make them available for general circulation. Individual sponsors may, however, authorize subsequent release of the material.

UNIVERSITY OF SOUTHAMPTON

INSTITUTE OF SOUND AND VIBRATION RESEARCH

DYNAMICS GROUP

Vibrational Analysis of a Non-Uniform One-Dimensional Structure Using a Wave Approach

by

S-K. Lee, B.R. Mace and M.J. Brennan

ISVR Technical Memorandum No: 918

September 2003

Authorised for issue by
Professor M.J. Brennan
Group Chairman

Abstract

The wave approach for the analysis of motion of a one-dimensional structure including bars and beams is reviewed. Matrix formulations, which include nearfield waves, of wave amplitudes, displacements and internal forces are developed. Reflection and transmission phenomena at various boundaries and discontinuities are also investigated. Two numerical methods, one using reflection, transmission and propagation matrices and the other using the transfer matrix approach, are considered. It is seen that, in the presence of nearfield waves, the transfer matrix method cannot be applied in the high frequency region due to numerical errors. The methods are applied to a non-uniform structure on the assumption that the structure is composed of small uniform sections. The numerical results show good agreement with analytical calculations in a bar.

Content

1. Introduction

Wave methods may be suitable to analyse the dynamic behaviour of a simple structure since they do not require powerful computing resources. However, most real structures are too complicated to apply wave methods easily. One typical case may be a one-dimensional structure which has non-uniform geometric shape or/and material properties.

The oldest problem related to a non-uniform structure is possibly the one in which a one-dimensional plane wave propagates in a horn which has a varying cross-sectional area. It has been found that the governing equation can be solved easily for several specific types, the so-called Salmon's family, which includes conical, exponential and catenoidal horns [1]. In vibration, Conway et al. [2] obtained an exact solution to the equation of motion for a conical beam in terms of Bessel functions and presented equations for finding the natural frequencies of such beams for four sets of boundary conditions. Mabie and Rogers [3, 4] used the same approach to study tapered beams with constant width and linearly varying thickness, or constant thickness and linearly varying width, or linearly varying width and thickness. Recently, there have been studies by Abrate [5] and Kumar et al. [6] to obtain exact solutions for bars and beams with specific geometric shapes.

Wave methods are based on the reflection, transmission and propagation of waves along a structure. Reference [7] contains a summary of previous work and some applications of the wave methods. Also, Mace [8] developed a matrix formulation including nearfield wave components.

Much work on non-uniform structures has been related to the transfer matrix method, which has been developed from the studies by Holzer and Myklestad [9]. Recently, Hodges et al. [10] studied the vibration of the tapered beam using the transfer matrix method. Langley [11]

studied the wave transmission through one-dimensional near periodic structures using the transfer matrix method. The numerical difficulties in the application of the transfer matrix method are discussed in reference [12].

In this report, wave methods are applied to the one-dimensional motion of a non-uniform structure. There are several typical structures that have one-dimensional motion in acoustic and vibration problems ? examples include a duct or muffler with effective cross-sectional dimension much less than a wavelength, a bar with axial vibration, a rod with torsional vibration and a beam with bending motion. In this report, the work is mainly concerned with axial motion in a bar and bending motion in a beam. However, the wave approach described in this report could be generally applied to any structure.

In section 2, general wave theory is reviewed. The matrix formulation for waves in a structure is introduced and the reflection, transmission and propagation matrices are defined for various conditions. Power carried by a wave and its reflection and transmission are also discussed.

In section 3, discrete wave models are developed for axial vibration and bending motion. Two methods, one using the reflection, transmission and propagation matrices and the other using the transfer matrix approach, are applied and a comparison of the results is carried out. It is also shown that the existence of the nearfield wave will induce numerical errors in the application of the transfer matrix method.

In section 4, the discrete wave models are expanded for continuous non-uniform structures. Numerical errors due to the discretization of the continuous system are discussed. As a real application, the axial vibration of a finite conical bar is investigated.

In section 5, the conclusion of this report is described.

Appendix A illustrates the influence of the nearfield wave for the case of a beam with two simply supported points. In appendix B, the transfer matrix method using reflection, transmission

and propagation matrices is developed. In appendix C, analytical methods applied to the axial vibration of a conical bar is described.

2. Review of wave approach

2.1 Introduction

In this section, the general wave approach for one-dimensional motion of a structure is reviewed. As mentioned in section 1, the work is mainly concerned with axial motion in a bar and bending motion in a beam. Also, the effects of shear deformation and rotary inertia in a beam are not considered and damping is not included. However, the methods discussed in this report could be generally applied to any structure [14].

In section 2.2, the wave equations and their solutions for a bar and a beam are reviewed. It is shown that the axial displacement of a uniform bar consists of two propagating wave components while the flexural displacement of a uniform beam consists of four wave components including two propagating and two nearfield waves.

In section 2.3, matrix formulations for the deflections and internal forces are developed. Wave propagation in the absence of a discontinuity is also expressed in matrix form.

In section 2.4, wave generation by a force and a moment are discussed. For various bars and beams, the relationships between the external forces and the amplitudes of the generated waves are derived.

If there is an impedance-mismatching component at a point, waves incident on the component are reflected and transmitted. In a section 2.5, reflections and transmissions of the waves are identified for various conditions.

In section 2.6, power (time averaged energy flow) carried by a wave is introduced. Also, power reflection and transmission coefficients satisfying the energy conservation law are defined.

2.2 Equation of motion

The axial displacement $u(x,t)$ for free vibration of a bar with varying cross-section at position x and time t is governed by the differential equation [13]

$$\frac{\partial}{\partial x}\left[EA(x)\frac{\partial u}{\partial x}\right]=\rho A(x)\frac{\partial^2 u}{\partial t^2} \tag{2.1}$$

where ρ is the density of bar and $EA(x)$ the axial stiffness, in which E is the modulus of elasticity and $A(x)$ the cross-sectional area.

Equation (2.1) can be easily solved if the cross-sectional area $A(x)$ is constant with position x. If a time dependence of the form $\exp(\mathrm{i}\omega t)$ is assumed but suppressed here for clarity, the solution for a uniform bar can be written as the sum of two propagating wave components, i.e.,

$$u(x)=a^{+}\mathrm{e}^{-\mathrm{i}k_l x}+a^{-}\mathrm{e}^{\mathrm{i}k_l x} \tag{2.2}$$

where a^{+} and a^{-} are the amplitudes of a positive-going wave and a negative-going wave, respectively, and may be complex. In equation (2.2), the wavenumber k_l is given by

$$k_l=\sqrt{\rho\omega^2/E} \tag{2.3}$$

and is real and positive, unless damping is present when it will have a negative imaginary part.

If the effects of shear deformation and rotary inertia can be neglected, the governing equation of flexural displacement $w(x,t)$ for free vibration of a beam with varying cross-section is given by [13]

$$\frac{\partial^2}{\partial x^2}\left[EI(x)\frac{\partial^2 w}{\partial x^2}\right]+\rho A(x)\frac{\partial^2 w}{\partial t^2}=0 \tag{2.4}$$

where $EI(x)$ is the bending stiffness and $I(x)$ is the second moment of area.

Similar to the axial vibration of a bar, equation (2.4) can also be easily solved if the cross-sectional area $A(x)$ and the second moment of area $I(x)$ are constant with position x.

However, the beam equation is of 4th order and, as a result, there are nearfield waves as well as propagating waves. The solution for a uniform beam can be written as the sum of four wave components, namely,

$$w(x) = a^{+}e^{-ik_b x} + a^{-}e^{ik_b x} + a_N^{+}e^{-k_b x} + a_N^{-}e^{k_b x} \tag{2.5}$$

where the subscript N refers to the nearfield wave components. In equation (2.5), the wavenumber k_b is given by

$$k_b = \sqrt[4]{\rho A\omega^2 / EI} \tag{2.6}$$

and is real and positive, unless damping is present when it will have a negative imaginary part. It should be noted that, unlike axial vibration, the wavenumber in bending motion depends on the specific geometric shape of the bar.

2.3 Wave amplitude vectors and propagation matrices

Introducing wave amplitude vectors, $\mathbf{a}^{+}$ for positive-going waves and $\mathbf{a}^{-}$ for negative-going waves, the displacement u of a uniform bar at a point can be written as

$$u = \mathbf{a}^{+} + \mathbf{a}^{-} \tag{2.7}$$

where the wave amplitude vectors are given by

$$\mathbf{a}^{+} = \{a^{+}\}, \qquad \mathbf{a}^{-} = \{a^{-}\} \tag{2.8a,b}$$

Also, the axial force P defined by $P = EA(\partial u/\partial x)$ where the convention is adopted of choosing a positive value of P to represent forces of tension can be written as

$$P = EA[-ik_l]\mathbf{a}^{+} + EA[ik_l]\mathbf{a}^{-} \tag{2.9}$$

If there is no impedance-mismatching component in the wave propagation path, the wave amplitude vectors at different positions on the bar are related by

$$\mathbf{a}^{+}(x_0 + x) = \mathbf{F}\,\mathbf{a}^{+}(x_0), \qquad \mathbf{a}^{-}(x_0 + x) = \mathbf{F}^{-1}\,\mathbf{a}^{-}(x_0) \tag{2.10a, b}$$

where $\mathbf{F}$ is called propagation matrix and, for axial vibration, is given by

$$\mathbf{F}=\left[\mathrm{e}^{-\mathrm{i}k_l x}\right] \tag{2.11}$$

The same concept can be applied to the bending motion. Then the wave amplitude vectors for a uniform beam are given by

$$\mathbf{a}^{+}=\begin{Bmatrix} a^{+} \\ a_N^{+} \end{Bmatrix}, \qquad \mathbf{a}^{-}=\begin{Bmatrix} a^{-} \\ a_N^{-} \end{Bmatrix} \tag{2.12a, b}$$

and the propagation matrix $\mathbf{F}$ is given by

$$\mathbf{F}=\begin{bmatrix} \mathrm{e}^{-\mathrm{i}k_b x} & 0 \\ 0 & \mathrm{e}^{-k_b x} \end{bmatrix} \tag{2.13}$$

It is convenient to group the displacement w and slope $\partial w/\partial x$ into the displacement vector $\mathbf{w}$ written as

$$\mathbf{w}=\begin{Bmatrix} w \\ \partial w/\partial x \end{Bmatrix}=\begin{bmatrix} 1 & 1 \\ -\mathrm{i}k_b & -k_b \end{bmatrix}\mathbf{a}^{+}+\begin{bmatrix} 1 & 1 \\ \mathrm{i}k_b & k_b \end{bmatrix}\mathbf{a}^{-} \tag{2.14}$$

Also, the shear force Q and bending moment M can be grouped into the internal force vector $\mathbf{f}$ written as

$$\mathbf{f}=\begin{Bmatrix} Q \\ M \end{Bmatrix}=EI\begin{bmatrix} \mathrm{i}k_b^{\,3} & -k_b^{\,3} \\ -k_b^{\,2} & k_b^{\,2} \end{bmatrix}\mathbf{a}^{+}+EI\begin{bmatrix} -\mathrm{i}k_b^{\,3} & k_b^{\,3} \\ -k_b^{\,2} & k_b^{\,2} \end{bmatrix}\mathbf{a}^{-} \tag{2.15}$$

with the definitions of shear force $Q=EI\left(\partial^3 w/\partial x^3\right)$ and bending moment $M=EI\left(\partial^2 w/\partial x^2\right)$ as shown in Figure 1.

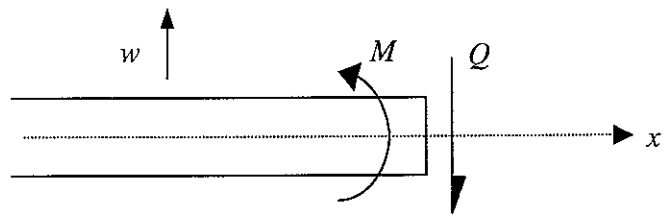

Figure 1. Definition of positive shear force and bending moment

2.4 Wave generated by line force or moment

If there is a semi-infinite uniform bar which is excited by a harmonic force $Fe^{i\omega t}$ at the end as shown in Figure 2, then a positive-going wave will be generated by the force. Since

$$-P(0) = F\,; \qquad \mathrm{i}EAk_l\mathbf{q}^+ = F \tag{2.16}$$

the wave amplitude vector $\mathbf{q}^+$ due to the external force can be written as

$$\mathbf{q}^+ = \left\{-\mathrm{i}\frac{F}{EAk_l}\right\} \tag{2.17}$$

It can be seen that the induced displacement of the bar lags in phase behind the external force by 90°. In the mirror case where the external force is applied in the negative direction at the right end of a semi-infinite bar, the negative-going wave amplitude $\mathbf{q}^-$ is given by

$$\mathbf{q}^- = \left\{\mathrm{i}\frac{F}{EAk_l}\right\} \tag{2.18}$$

It can be seen that equation (2.18) is identical to equation (2.17) except the sign since the direction of the excitation force is reversed.

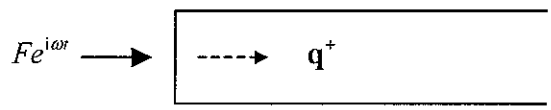

Figure 2. Semi-infinite bar with a harmonic force applied at the end.

Similar to the case of axial vibration under a harmonic force, consider an infinite uniform beam which is excited by a harmonic force $Fe^{i\omega t}$ at a point as shown in Figure 3. If positive-going wave amplitude vector is $\mathbf{q}^+$ and negative-going wave amplitude vector is $\mathbf{q}^-$, the displacement vector $\mathbf{w}$ on both sides of the point can be written as

$$\mathbf{w}_1 = \begin{bmatrix} 1 & 1 \\ \mathrm{i}k_b & k_b \end{bmatrix}\mathbf{q}^-, \qquad \mathbf{w}_2 = \begin{bmatrix} 1 & 1 \\ -\mathrm{i}k_b & -k_b \end{bmatrix}\mathbf{q}^+ \tag{2.19a, b}$$

and the internal force vector $\mathbf{f}$ as

$$\mathbf{f}_1 = EI\begin{bmatrix} -\mathrm{i}k_b^{\,3} & k_b^{\,3} \\ -k_b^{\,2} & k_b^{\,2} \end{bmatrix}\mathbf{q}^-, \qquad \mathbf{f}_2 = EI\begin{bmatrix} \mathrm{i}k_b^{\,3} & -k_b^{\,3} \\ -k_b^{\,2} & k_b^{\,2} \end{bmatrix}\mathbf{q}^+ \tag{2.20a, b}$$

where the subscripts 1 and 2 refer to the left-hand and right-hand sides of the point force, respectively. Since the continuity and equilibrium conditions at the point are given by

$$\begin{aligned} \mathbf{w}_1 &= \mathbf{w}_2 \\ -\mathbf{f}_1 + \mathbf{f}_2 &= \begin{Bmatrix} F \\ 0 \end{Bmatrix} \end{aligned} \tag{2.21a, b}$$

combining equation (2.19) with (2.21) gives [15]

$$\mathbf{q}^+ = \mathbf{q}^- = -\frac{F}{4EIk_b^{\,3}}\begin{Bmatrix} \mathrm{i} \\ 1 \end{Bmatrix} \tag{2.22}$$

It can be seen that the amplitude of the external force is equally distributed among each wave component and the induced displacement lags in phase behind the force by 135°.

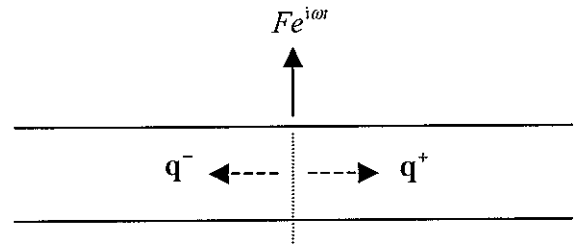

Figure 3. Infinite beam with a harmonic force applied at a point.

If a beam is semi-infinite and is excited by a harmonic force $Fe^{i\omega t}$ at the left-hand end as shown in Figure 4, the equilibrium conditions at the end are given by

$$\mathbf{f} = \begin{Bmatrix} F \\ 0 \end{Bmatrix} \tag{2.23}$$

Therefore the positive-going wave amplitude $\mathbf{q}^+$ of this case is given by

$$\mathbf{q}^{+} = -\frac{(1+\mathrm{i})F}{2EIk_b^{\,3}}\begin{Bmatrix}1\\1\end{Bmatrix} \tag{2.24}$$

It can be seen that the amplitude of the external force is equally distributed among each wave component and the induced displacement also lags in phase behind the force by 135°. In the mirror case where the external force is applied at the right-hand end, the negative-going wave amplitude $\mathbf{q}^{-}$ is identical to equation (2.24), namely,

$$\mathbf{q}^{-} = -\frac{(1+\mathrm{i})F}{2EIk_b^{\,3}}\begin{Bmatrix}1\\1\end{Bmatrix} \tag{2.25}$$

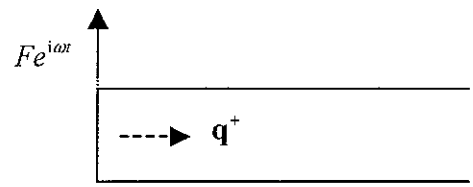

Figure 4. Semi-infinite beam with a harmonic force applied at the end.

Besides a force, a moment can also be considered as a source generating bending motion. If a counter-clockwise moment is applied to an infinite beam at a point as shown in Figure 5, the continuity and equilibrium conditions are given by

$$\begin{aligned}\mathbf{w}_1 &= \mathbf{w}_2\\ \mathbf{f}_1 - \mathbf{f}_2 &= \begin{Bmatrix}0\\M\end{Bmatrix}\end{aligned} \tag{2.26a, b}$$

Therefore the wave amplitude vectors are given by [15]

$$\mathbf{q}^{+} = -\mathbf{q}^{-} = \frac{M}{4EIk_b^{\,2}}\begin{Bmatrix}1\\-1\end{Bmatrix} \tag{2.27}$$

It can be seen that the amplitude of the external force is equally distributed among each wave component and the resulting displacement at the position of the source is zero. Also, it should be noted that the induced slope (or, rotation) lags in phase behind the moment by 45°.

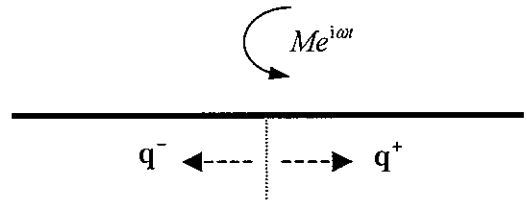

Figure 5. Infinite beam with a harmonic moment applied at a point.

For a semi-infinite beam under a counter-clockwise moment at the left end, the wave amplitude vector is given by

$$\mathbf{q}^+ = \frac{(1+\mathrm{i})M}{2EIk_b^{\,2}} \begin{Bmatrix} 1 \\ \mathrm{i} \end{Bmatrix} \tag{2.28}$$

and, for a semi-infinite beam under a counter-clockwise moment at the right end, the wave amplitude vector is given by

$$\mathbf{q}^- = -\frac{(1+\mathrm{i})M}{2EIk_b^{\,2}} \begin{Bmatrix} 1 \\ \mathrm{i} \end{Bmatrix} \tag{2.29}$$

2.5 Reflection and transmission matrices

If there are waves incident upon a boundary of a structure, reflected waves will be set up, the amplitudes of which can be determined by considering the boundary conditions. In the case where there is a discontinuity at a point on the structure, incident waves on the discontinuity will give rise to transmitted waves together with reflected waves. The amplitudes of the reflected and transmitted waves can be determined by considering continuity and equilibrium conditions at the discontinuity.

The amplitude of the reflected and transmitted waves can be found in terms of reflection and transmission matrices. In this section, these matrices are determined for various boundary conditions and discontinuities.

2.5.1 The bar

If there is a semi-infinite bar with a boundary consisting of a translational dynamic stiffness $\bar{K}_T$ as shown in Figure 6, the equilibrium condition at the end is given by

$$P = -\bar{K}_T u \tag{2.30}$$

Combining equation (2.30) with equations (2.7) and (2.9) yields

$$EA\left(-\mathrm{i}k_l\mathbf{a}^+ + \mathrm{i}k_l\mathbf{a}^-\right) = -\bar{K}_T\left(\mathbf{a}^+ + \mathbf{a}^-\right) \tag{2.31}$$

where $\mathbf{a}^+$ is the incident wave amplitude vector and $\mathbf{a}^-$ is the reflected wave amplitude vector. Therefore the reflection matrix $\mathbf{R}$ of the boundary is given by

$$\mathbf{R} = \left[\frac{1+\mathrm{i}K_T}{1-\mathrm{i}K_T}\right] \tag{2.32}$$

where the dimensionless stiffness $K_T = \bar{K}_T / EAk_l$ is introduced. For two special cases - namely, clamped ($\bar{K}_T \to \infty$) and free ($\bar{K}_T = 0$) boundary conditions, the reflection matrices are given by

$$\mathbf{R}_c = [-1], \qquad \mathbf{R}_f = [1] \tag{2.33a, b}$$

where the subscript c and f refer to the boundary conditions, respectively.

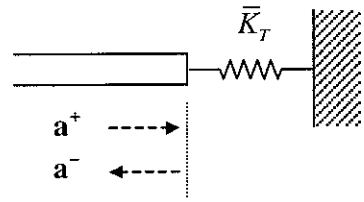

Figure 6. Semi-infinite bar with a boundary consisting of a translational dynamic stiffness

If two identical semi-infinite bars are connected by a translational dynamic stiffness $\bar{K}_T$ as shown in Figure 7, the continuity and equilibrium conditions are given by

$$\begin{aligned} P_1 &= P_2 \\ P_1 &= \bar{K}_T\left(u_2 - u_1\right) \end{aligned} \tag{2.34a, b}$$

where the subscripts 1 and 2 refer to the left-hand and right-hand sides of the stiffness, respectively. Combining equation (2.34) with equations (2.7) and (2.9) gives the reflection and transmission matrices for this case, namely,

$$\mathbf{R}=\left[\frac{1}{1-\mathrm{i}2K_T}\right], \qquad \mathbf{T}=\left[-\frac{\mathrm{i}2K_T}{1-\mathrm{i}2K_T}\right] \tag{2.35a, b}$$

It can be seen that there is no reflection if $\bar{K}_T \to \infty$ (rigid connection) and there is no transmission if $\bar{K}_T = 0$ (no connection).

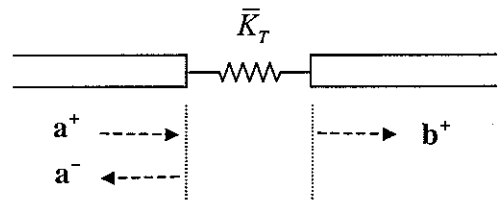

Figure 7. Two identical semi-infinite bars connected by a translational dynamic stiffness

If two semi-infinite bars with different geometric shapes or/and material properties are directly connected as shown in Figure 8, the continuity and equilibrium conditions at the junction are given by

$$\begin{aligned} u_1 &= u_2 \\ P_1 &= P_2 \end{aligned} \tag{2.36a, b}$$

where the subscripts 1 and 2 refer to the left-hand and right-hand sides of the junction, respectively. Combining equation (2.36) with equations (2.7) and (2.9) gives the reflection and transmission matrices for this case, namely,

$$\mathbf{R}=\left[\frac{1-\gamma}{1+\gamma}\right], \qquad \mathbf{T}=\left[\frac{2}{1+\gamma}\right] \tag{2.37a, b}$$

where $\gamma = (EAk_l)_2/(EAk_l)_1$ represents the ratio of the axial wave impedances of the two bars. For extreme cases where $\gamma \to \infty$ and $\gamma \to 0$, the reflection matrices are identical to those in equation (2.33).

If only the cross-sectional areas of the two bars are different, then the reflection and transmission matrices can be expressed in terms of the cross-sectional areas and reduce to

$$\mathbf{R} = \left[\frac{A_1 - A_2}{A_1 + A_2}\right], \qquad \mathbf{T} = \left[\frac{2A_1}{A_1 + A_2}\right] \tag{2.38}$$

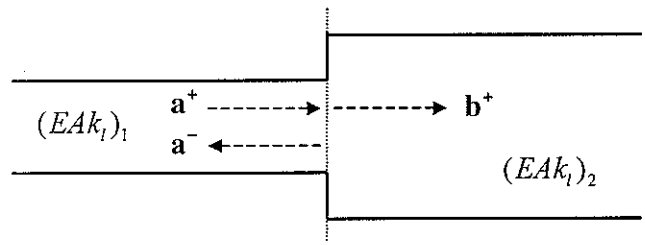

Figure 8. Two semi-infinite bars with different geometric shapes or/and material properties.

2.5.2 The beam

If there is a semi-infinite beam with a boundary consisting of translational and rotational dynamic stiffnesses $\bar{K}_T$ and $\bar{K}_R$ as shown in Figure 9, the equilibrium condition at the end is given by

$$\mathbf{f} = \begin{bmatrix} \bar{K}_T & 0 \\ 0 & -\bar{K}_R \end{bmatrix} \mathbf{w} \tag{2.39}$$

Combining equation (2.39) with equations (2.14) and (2.15), the reflection matrix $\mathbf{R}$ of the boundary is determined to be [8]

$$\mathbf{R} = \begin{bmatrix} 1-\mathrm{i}K_T & \mathrm{i}(1-K_T) \\ -1+\mathrm{i}K_R & 1+K_R \end{bmatrix}^{-1} \begin{bmatrix} 1+\mathrm{i}K_T & \mathrm{i}(1+K_T) \\ 1+\mathrm{i}K_R & -1+K_R \end{bmatrix} \tag{2.40}$$

where the dimensionless stiffnesses $K_T = \bar{K}_T / EIk_b^3$ and $K_R = \bar{K}_R / EIk_b$ are introduced. For three common cases of interest - namely, simply supported, clamped and free ends, the reflection matrix $\mathbf{R}$ reduces to

$$\mathbf{R}_s = \begin{bmatrix} -1 & 0 \\ 0 & -1 \end{bmatrix}, \qquad \mathbf{R}_c = \begin{bmatrix} -\mathrm{i} & -(1+\mathrm{i}) \\ -(1-\mathrm{i}) & \mathrm{i} \end{bmatrix}, \qquad \mathbf{R}_f = \begin{bmatrix} -\mathrm{i} & (1+\mathrm{i}) \\ (1-\mathrm{i}) & \mathrm{i} \end{bmatrix} \tag{2.41a, b, c}$$

where the subscripts s, c and f refer the boundary conditions, respectively.

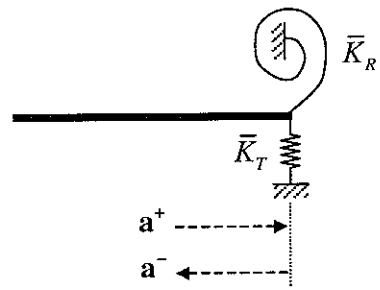

Figure 9. Semi-infinite beam with a boundary consisting of generalized dynamic stiffnesses.

Consider an infinite beam which is supported by a point (or localized) impedance mismatching component like a spring as shown in Figure 10. The continuity and equilibrium conditions at the discontinuity are given by

$$\begin{aligned} \mathbf{w}_1 &= \mathbf{w}_2 \\ \mathbf{f}_1 - \mathbf{f}_2 &= \begin{bmatrix} \bar{K}_T & 0 \\ 0 & -\bar{K}_R \end{bmatrix} \mathbf{w}_{1 \text{ or } 2} \end{aligned} \tag{2.42a, b}$$

where the subscripts 1 and 2 refer to the left-hand and right-hand sides of the discontinuity, respectively. Combining equation (2.42) with equations (2.14) and (2.15), the reflection and transmission matrices of the discontinuity are determined to be [8]

$$\mathbf{R} = \mu\mathbf{c} - \eta\mathbf{d}, \qquad \mathbf{T} = \mathbf{I} + \mu\mathbf{c} - \eta\mathbf{d} \tag{2.43a, b}$$

where $\mathbf{I}$ is the identity matrix and

$$\mathbf{c} = \begin{bmatrix} \mathrm{i} & \mathrm{i} \\ 1 & 1 \end{bmatrix}, \quad \mathbf{d} = \begin{bmatrix} -\mathrm{i} & -1 \\ \mathrm{i} & 1 \end{bmatrix}, \quad \mu = \frac{K_T}{4-(1+\mathrm{i})K_T}, \quad \eta = \frac{K_R}{4+(1-\mathrm{i})K_R} \tag{2.44a, b, c, d}$$

The parameters μ and η represent the effects of the translational and rotational constraints, respectively, and are in general frequency dependent. For a simply supported point (namely, $\bar{K}_T \to \infty$ and $\bar{K}_R = 0$), the reflection and transmission matrices reduce to

$$\mathbf{R} = \frac{1}{1-\mathrm{i}} \begin{bmatrix} -1 & -1 \\ \mathrm{i} & \mathrm{i} \end{bmatrix}, \qquad \mathbf{T} = \frac{1}{1-\mathrm{i}} \begin{bmatrix} -\mathrm{i} & -1 \\ \mathrm{i} & 1 \end{bmatrix} \tag{2.45a, b}$$

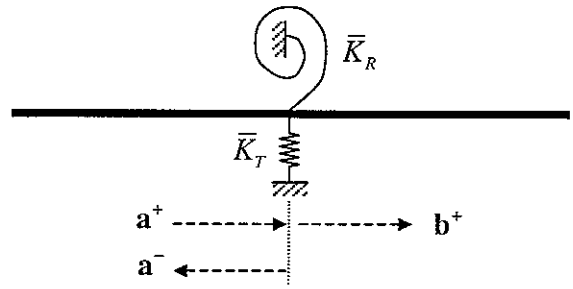

Figure 10. Point supported, infinite beam.

Consider the case where two semi-infinite beams with different geometric shapes and/or material properties are directly connected as shown in Figure 11. The displacement, slope, bending moment and shear force are all continuous at the junction, namely,

$$\begin{aligned} \mathbf{w}_1 &= \mathbf{w}_2 \\ \mathbf{f}_1 &= \mathbf{f}_2 \end{aligned} \tag{2.46a, b}$$

where the subscripts 1 and 2 refer to the left-hand and right-hand side of the junction, respectively. Combining equation (2.46) with equations (2.14) and (2.15), the reflection and transmission matrices are determined to be [8]

$$\begin{aligned} \mathbf{R} &= \frac{2}{\Delta}\begin{bmatrix} -2(\beta^2-1)\gamma - \mathrm{i}\beta(1-\gamma)^2 & (1+\mathrm{i})\beta(1-\gamma^2) \\ (1-\mathrm{i})\beta(1-\gamma^2) & -2(\beta^2-1)\gamma + \mathrm{i}\beta(1-\gamma)^2 \end{bmatrix}, \\ \mathbf{T} &= \frac{4}{\Delta}\begin{bmatrix} (1+\beta)(1+\gamma) & -(1-\mathrm{i}\beta)(1-\gamma) \\ -(1+\mathrm{i}\beta)(1-\gamma) & (1+\beta)(1+\gamma) \end{bmatrix} \end{aligned} \tag{2.47a, b}$$

where $\Delta = (1+\beta)^2(1+\gamma)^2 - (1+\beta^2)(1-\gamma)^2$. The parameters

$$\beta = k_{b,2}/k_{b,1}, \qquad \gamma = (EIk_b^{\,2})_2/(EIk_b^{\,2})_1 \tag{2.48a, b}$$

represent the ratios of wavenumber and bending wave impedance, respectively. It should be noted that the transmission and reflection matrices are independent of frequency.

When the cross-section shapes of the two beams are all rectangular and the two beams are identical except for the thickness, the phase of R_{11} tends to $-\pi/2$ as the thickness difference increases [8]. If the two beams are identical except for the width, the reflection and transmission

matrices are only a function of the ratio of the width change since the ratio of the wavenumbers β is unity so that

$$\mathbf{R}=\frac{2}{\Delta}\begin{bmatrix} -\mathrm{i}(1-\gamma)^2 & (1+\mathrm{i})(1-\gamma^2) \\ (1-\mathrm{i})(1-\gamma^2) & \mathrm{i}(1-\gamma)^2 \end{bmatrix},$$
$$\mathbf{T}=\frac{4}{\Delta}\begin{bmatrix} 2(1+\gamma) & -(1-\mathrm{i})(1-\gamma) \\ -(1+\mathrm{i})(1-\gamma) & 2(1+\gamma) \end{bmatrix} \tag{2.49a, b}$$

where $\Delta=2(\gamma^2+6\gamma+1)$ and $\gamma=b_2/b_1$ in which b refers to the width. It can be seen that the phases of all coefficients are independent of the ratio of the width changes γ and, in particular, the phase of R_{11} is $-\pi/2$.

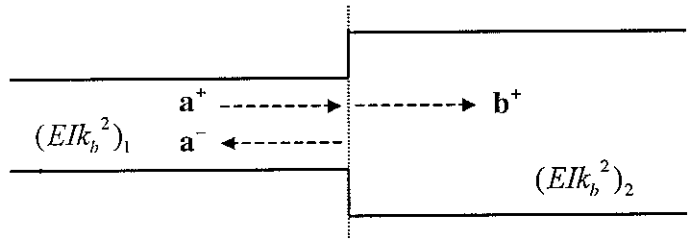

Figure 11. Two semi-infinite beams with different geometric shapes or/and material properties.

2.6 Power reflection and transmission coefficients

For two oscillatory quantities with complex amplitudes α and β and time dependence $\exp(+\mathrm{i}\omega t)$, the time-averaged product of the two quantities is given by

$$\begin{aligned}\left\langle \mathrm{Re}\left\{\alpha e^{+\mathrm{i}\omega t}\right\}\cdot \mathrm{Re}\left\{\beta e^{+\mathrm{i}\omega t}\right\}\right\rangle &= \left\langle \frac{1}{2}\left(\alpha e^{+\mathrm{i}\omega t}+\alpha^* e^{-\mathrm{i}\omega t}\right)\cdot\frac{1}{2}\left(\beta e^{+\mathrm{i}\omega t}+\beta^* e^{-\mathrm{i}\omega t}\right)\right\rangle \\ &= \frac{1}{4}\left\langle \alpha\beta e^{+\mathrm{i}2\omega t}+\alpha\beta^*+\alpha^*\beta+\alpha^*\beta^* e^{-\mathrm{i}2\omega t}\right\rangle \\ &= \frac{1}{4}\left(\alpha\beta^*+\alpha^*\beta\right) \\ &= \frac{1}{2}\mathrm{Re}\left(\alpha\beta^*\right)\end{aligned} \tag{2.50}$$

where the bracket $\langle\ \rangle$ refers to the time average and the superscript * means the complex

conjugate operator .

For axial motion in a bar, the time-averaged power is the product of the axial force and the velocity given by [7]

$$\Pi = \left\langle -\mathrm{Re}\{P(x,t)\} \cdot \mathrm{Re}\left\{\frac{\partial u(x,t)}{\partial t}\right\} \right\rangle \tag{2.51}$$

The power in a bar can thus be written as

$$\Pi = \frac{1}{2}\mathrm{Re}\left\{\mathrm{i}\omega u^{*}(x) P(x)\right\} \tag{2.52}$$

If the displacement $u(x)$ consists only of a positive-going wave, namely $u(x) = a^{+}e^{-ik_l x}$, then the power is given by

$$\begin{aligned} \Pi &= \frac{1}{2}\mathrm{Re}\left\{\mathrm{i}\omega (a^{+})^{*} e^{ik_l x} EA(-\mathrm{i}k_l) a^{+} e^{-ik_l x}\right\} \\ &= \frac{1}{2}\omega EAk_l \left|a^{+}\right|^2 \\ &= \frac{1}{2}\rho A\omega^2 \left|a^{+}\right|^2 c_l \end{aligned} \tag{2.53}$$

where c_l refers to longitudinal wavespeed given by $c_l = \sqrt{E/\rho}$. It can be seen that power is proportional to the longitudinal wavespeed. Similarly, if displacement is given by a negative-going wave, namely, $u(x) = a^{-}e^{+ik_l x}$, then the power is given by

$$\begin{aligned} \Pi &= -\frac{1}{2}\omega EAk_l \left|a^{-}\right|^2 \\ &= -\frac{1}{2}\rho A\omega^2 \left|a^{-}\right|^2 c_l \end{aligned} \tag{2.54}$$

For bending motion in a beam, power is the sum of the force contribution and the moment contribution, namely [7],

$$\Pi = \left\langle \mathrm{Re}\{Q\} \cdot \mathrm{Re}\left\{\frac{\partial w}{\partial t}\right\} - \mathrm{Re}\{M\} \cdot \mathrm{Re}\left\{\frac{\partial}{\partial t}\left(\frac{\partial w}{\partial x}\right)\right\} \right\rangle \tag{2.55}$$

The power in a beam can thus be written as

$$\Pi = \frac{1}{2}\mathrm{Re}\left\{-\mathrm{i}\omega w^{*}Q + \mathrm{i}\omega (w')^{*} M\right\} \tag{2.56}$$

where the prime denotes differentiation with respect to x.

If the displacement $w(x)$ is given by positive-going waves as $w(x) = a^{+}e^{-ik_b x} + a_N^{+}e^{-k_b x}$, then the force contribution and the moment contribution are written as

$$\begin{aligned} w^{*}Q &= EIk_b{}^{3}\left\{\mathrm{i}\left|a^{+}\right|^{2} - \left|a_N^{+}\right|^{2} e^{-2k_b x} - \varepsilon(x) + \mathrm{i}\varepsilon^{*}(x)\right\} \\ w'^{*}M &= EIk_b{}^{3}\left\{-\mathrm{i}\left|a^{+}\right|^{2} - \left|a_N^{+}\right|^{2} e^{-2k_b x} + \mathrm{i}\varepsilon(x) + \varepsilon^{*}(x)\right\} \end{aligned} \tag{2.57a, b}$$

where $\varepsilon(x)$ is given by

$$\varepsilon(x) = (a^{+})^{*} a_N^{+} e^{\mathrm{i}k_b x} e^{-k_b x} \tag{2.58}$$

Therefore the power carried by the positive-going waves reduces to

$$\begin{aligned} \Pi &= \omega EIk_b{}^{3}\left|a^{+}\right|^{2} \\ &= \frac{1}{2}\rho A\omega^{2}\left|a^{+}\right|^{2} c_g \end{aligned} \tag{2.59}$$

where c_g is the group velocity of the wave defined by $c_g = d\omega/dk$. Equation (2.59) shows that only the propagating wave transfers energy and there is no energy transferred by the nearfield wave or by the interactions between the propagating wave and the nearfield wave. However, energy can be transferred by the interaction between nearfield waves [18]. The power associated with interaction between nearfield waves is not considered in this report.

Similarly, if the displacement $w(x)$ consists only of negative-going waves, namely, $w(x) = a^{-}e^{ik_b x} + a_N^{-}e^{k_b x}$, then the power is given by

$$\begin{aligned} \Pi &= -\omega EIk_b{}^{3}\left|a^{-}\right|^{2} \\ &= -\frac{1}{2}\rho A\omega^{2}\left|a^{-}\right|^{2} c_g \end{aligned} \tag{2.60}$$

If waves are incident on a discontinuity, the power reflection coefficient ϱ and power transmission coefficient τ at the discontinuity can be defined by

$$\varrho = -\frac{\Pi_{reflected}}{\Pi_{incident}}, \qquad \tau = \frac{\Pi_{transmitted}}{\Pi_{incident}} \tag{2.61a, b}$$

If there is no energy dissipation in the wave path, the power reflection and transmission coefficients should satisfy

$$\varrho + \tau = 1 \tag{2.62}$$

For axial vibration, the power reflection and transmission coefficients at a discontinuity are given by

$$\varrho = \frac{\left|a^-\right|^2}{\left|a^+\right|^2}, \qquad \tau = \frac{(EAk_l)_2}{(EAk_l)_1}\frac{\left|b^+\right|^2}{\left|a^+\right|^2} \tag{2.63a, b}$$

where a^+, a^- and b^+ refer to the incident, reflected and transmitted propagating wave amplitudes, respectively, and the subscripts 1 and 2 refer to left-hand and right-hand side of the discontinuity, respectively.

For bending motion, the power reflection and transmission coefficients at a discontinuity are given by

$$\varrho = \frac{\left|a^-\right|^2}{\left|a^+\right|^2}, \qquad \tau = \frac{(EIk_b^{\,3})_2}{(EIk_b^{\,3})_1}\frac{\left|b^+\right|^2}{\left|a^+\right|^2} \tag{2.64a, b}$$

2.7 Summary

In this section, the general wave theory for a one-dimensional structure has been reviewed. In section 2.2, the wave equations and their solutions for a bar and a beam were introduced. It was shown that the displacement of a uniform bar can be described as a sum of two propagating wave components while the displacement of a uniform beam can be described as a sum of two

propagating waves and two nearfield waves.

In section 2.3, the matrix formulations for wave amplitudes, deflections and internal forces were introduced. Also, the propagation matrix was defined in the absence of a discontinuity.

In section 2.4, wave generation by an external force or moment was discussed for various conditions. It was shown that the amplitude of the external force/moment is equally distributed among each wave component.

In section 2.5, the reflection and transmission of waves was investigated for various conditions. The reflection and transmission matrices defined in this section 2.5 can be directly used to calculate the reflected and transmitted wave amplitudes without considering the continuity and equilibrium conditions of the discontinuity.

In section 2.6, the power carried by longitudinal and flexural waves was determined. It was shown that power is proportional to the group velocity of a structure. It was also shown that power is a function of the amplitude of the propagating wave if there is no interaction between nearfield waves.

3. Discretely non-uniform structures

3.1 Introduction

In this section, the wave methods described in section 2 are applied to a one-dimensional non-uniform structure. There may be many types of non-uniformity including changes in the material properties and the geometric shape. Attention is confined to two discrete changes in cross-sectional area in a region. This is a very simple case since most real structures are far more complicated. However, it will serve as the basis for the analysis of complex non-uniform structures.

In section 3.2, the way in which waves are reflected, transmitted and propagate through the two cross-sectional area changes in a general structure is investigated. Two methods are discussed in the application - one relates wave amplitudes to reflection, transmission and propagation matrices and the other is the transfer matrix method as described in Appendix B.

In section 3.3, the axial waves in an infinite bar with two cross-sectional area changes are considered. This is similar to a one-dimensional acoustic duct, so the analysis could be directly applied to this situation.

In section 3.4, the bending waves in an infinite beam with two changes in cross-section are considered. Unlike axial motion, nearfield waves exist in bending motion, which makes the analysis somewhat different to that for axial motion. One of the difficulties of the transfer matrix method is also seen in this application.

3.2 Wave analysis

3.2.1 Reflection, transmission and propagation matrices

Consider an infinite one-dimensional structure with two cross-sectional area changes as shown in Figure 12. The length between the two junctions is denoted by L and the cross-sectional areas by A_1, A_2 and A_3, respectively. As shown in Appendix A, the wave amplitudes at the two junctions are related by reflection, transmission and propagation matrices, $\mathbf{R}$, $\mathbf{T}$ and $\mathbf{F}$ by

$$\begin{aligned}
\mathbf{b}^+ &= [\mathbf{I} - \hat{\mathbf{R}}_1\mathbf{F}\mathbf{R}_2\mathbf{F}]^{-1}\mathbf{T}_1\mathbf{a}^+ \\
\mathbf{c}^+ &= \mathbf{F}[\mathbf{I} - \hat{\mathbf{R}}_1\mathbf{F}\mathbf{R}_2\mathbf{F}]^{-1}\mathbf{T}_1\mathbf{a}^+ \\
\mathbf{c}^- &= \mathbf{R}_2\mathbf{F}[\mathbf{I} - \hat{\mathbf{R}}_1\mathbf{F}\mathbf{R}_2\mathbf{F}]^{-1}\mathbf{T}_1\mathbf{a}^+ \\
\mathbf{b}^- &= \mathbf{F}\mathbf{R}_2\mathbf{F}[\mathbf{I} - \hat{\mathbf{R}}_1\mathbf{F}\mathbf{R}_2\mathbf{F}]^{-1}\mathbf{T}_1\mathbf{a}^+
\end{aligned} \qquad (3.1a, b, c, d)$$

and

$$\begin{aligned}
\mathbf{a}^- &= \mathbf{R}_1\mathbf{a}^+ + \hat{\mathbf{T}}_1\mathbf{F}\mathbf{R}_2\mathbf{F}[\mathbf{I} - \hat{\mathbf{R}}_1\mathbf{F}\mathbf{R}_2\mathbf{F}]^{-1}\mathbf{T}_1\mathbf{a}^+ \\
\mathbf{d}^+ &= \mathbf{T}_2\mathbf{F}[\mathbf{I} - \hat{\mathbf{R}}_1\mathbf{F}\mathbf{R}_2\mathbf{F}]^{-1}\mathbf{T}_1\mathbf{a}^+
\end{aligned} \qquad (3.2a, b)$$

where the subscripts 1 and 2 refer to the junctions, respectively, and the superscripts $\cap$ are used to indicate the reflection and transmission matrices when the wave is incident from the right-hand side of the junction.

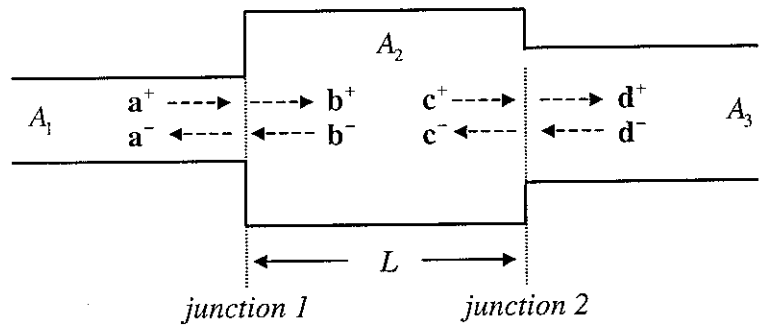

Figure 12. An infinite structure with two changes in cross-sectional area.

Note that the reflection and transmission matrices at the two junctions are not identical. Also, the matrices $\hat{\mathbf{R}}$ and $\hat{\mathbf{T}}$ are not in general identical to the matrices $\mathbf{R}$ and $\mathbf{T}$.

The net reflection and transmission matrices, $\mathbf{R}_T$ and $\mathbf{T}_T$, in this case are the terms multiplying the incident wave $\mathbf{a}^+$ in equation (3.2), namely,

$$\begin{aligned} \mathbf{a}^- &= \mathbf{R}_T\mathbf{a}^+; \qquad \mathbf{R}_T = \mathbf{R}_1 + \hat{\mathbf{T}}_1\mathbf{F}\mathbf{R}_2\mathbf{F}[\mathbf{I} - \hat{\mathbf{R}}_1\mathbf{F}\mathbf{R}_2\mathbf{F}]^{-1}\mathbf{T}_1 \\ \mathbf{d}^+ &= \mathbf{T}_T\mathbf{a}^+; \qquad \mathbf{T}_T = \mathbf{T}_2\mathbf{F}[\mathbf{I} - \hat{\mathbf{R}}_1\mathbf{F}\mathbf{R}_2\mathbf{F}]^{-1}\mathbf{T}_1 \end{aligned} \tag{3.3a, b}$$

3.2.2 Transfer matrix method

The transfer matrix method, which is described in Appendix B, can also be applied to this case. Now, the relevant wave amplitudes are given by

$$\begin{aligned} \begin{Bmatrix} \mathbf{b}^+ \\ \mathbf{b}^- \end{Bmatrix} &= \begin{bmatrix} \mathbf{T}_1 - \hat{\mathbf{R}}_1\hat{\mathbf{T}}_1^{-1}\mathbf{R}_1 & \hat{\mathbf{R}}_1\hat{\mathbf{T}}_1^{-1} \\ -\hat{\mathbf{T}}_1^{-1}\mathbf{R}_1 & \hat{\mathbf{T}}_1^{-1} \end{bmatrix} \begin{Bmatrix} \mathbf{a}^+ \\ \mathbf{a}^- \end{Bmatrix} \\ \begin{Bmatrix} \mathbf{c}^+ \\ \mathbf{c}^- \end{Bmatrix} &= \begin{bmatrix} \mathbf{F} & 0 \\ 0 & \mathbf{F}^{-1} \end{bmatrix} \begin{bmatrix} \mathbf{T}_1 - \hat{\mathbf{R}}_1\hat{\mathbf{T}}_1^{-1}\mathbf{R}_1 & \hat{\mathbf{R}}_1\hat{\mathbf{T}}_1^{-1} \\ -\hat{\mathbf{T}}_1^{-1}\mathbf{R}_1 & \hat{\mathbf{T}}_1^{-1} \end{bmatrix} \begin{Bmatrix} \mathbf{a}^+ \\ \mathbf{a}^- \end{Bmatrix} \end{aligned} \tag{3.4a, b}$$

and

$$\begin{Bmatrix} \mathbf{d}^+ \\ \mathbf{d}^- \end{Bmatrix} = \begin{bmatrix} \mathbf{T}_2 - \hat{\mathbf{R}}_2\hat{\mathbf{T}}_2^{-1}\mathbf{R}_2 & \hat{\mathbf{R}}_2\hat{\mathbf{T}}_2^{-1} \\ -\hat{\mathbf{T}}_2^{-1}\mathbf{R}_2 & \hat{\mathbf{T}}_2^{-1} \end{bmatrix} \begin{bmatrix} \mathbf{F} & 0 \\ 0 & \mathbf{F}^{-1} \end{bmatrix} \begin{bmatrix} \mathbf{T}_1 - \hat{\mathbf{R}}_1\hat{\mathbf{T}}_1^{-1}\mathbf{R}_1 & \hat{\mathbf{R}}_1\hat{\mathbf{T}}_1^{-1} \\ -\hat{\mathbf{T}}_1^{-1}\mathbf{R}_1 & \hat{\mathbf{T}}_1^{-1} \end{bmatrix} \begin{Bmatrix} \mathbf{a}^+ \\ \mathbf{a}^- \end{Bmatrix} \tag{3.5}$$

Equation (3.5) can be more simply rewritten as

$$\begin{Bmatrix} \mathbf{d}^+ \\ \mathbf{d}^- \end{Bmatrix} = \begin{bmatrix} \mathcal{T}_{11} & \mathcal{T}_{12} \\ \mathcal{T}_{21} & \mathcal{T}_{22} \end{bmatrix} \begin{Bmatrix} \mathbf{a}^+ \\ \mathbf{a}^- \end{Bmatrix} \tag{3.6}$$

where the transfer matrix $\mathcal{T}$ is given by

$$\mathcal{T} = \begin{bmatrix} \mathcal{T}_{11} & \mathcal{T}_{12} \\ \mathcal{T}_{21} & \mathcal{T}_{22} \end{bmatrix} = \begin{bmatrix} \mathbf{T}_2 - \hat{\mathbf{R}}_2\hat{\mathbf{T}}_2^{-1}\mathbf{R}_2 & \hat{\mathbf{R}}_2\hat{\mathbf{T}}_2^{-1} \\ -\hat{\mathbf{T}}_2^{-1}\mathbf{R}_2 & \hat{\mathbf{T}}_2^{-1} \end{bmatrix} \begin{bmatrix} \mathbf{F} & 0 \\ 0 & \mathbf{F}^{-1} \end{bmatrix} \begin{bmatrix} \mathbf{T}_1 - \hat{\mathbf{R}}_1\hat{\mathbf{T}}_1^{-1}\mathbf{R}_1 & \hat{\mathbf{R}}_1\hat{\mathbf{T}}_1^{-1} \\ -\hat{\mathbf{T}}_1^{-1}\mathbf{R}_1 & \hat{\mathbf{T}}_1^{-1} \end{bmatrix} \tag{3.7}$$

In this case, there are no negative-going waves on the right-hand side of the junction 2 since the

structure is assumed to be infinite and hence $\mathbf{d}^- = 0$. Therefore the reflected wave amplitude vector $\mathbf{a}^-$ and the transmitted wave amplitude vector $\mathbf{d}^+$ can be written as

$$\begin{aligned} \mathbf{a}^- &= -\mathcal{T}_{22}^{-1}\mathcal{T}_{21}\mathbf{a}^+ \\ \mathbf{d}^+ &= \left(\mathcal{T}_{11} - \mathcal{T}_{12}\mathcal{T}_{22}^{-1}\mathcal{T}_{21}\right)\mathbf{a}^+ \end{aligned} \tag{3.8a, b}$$

and the net reflection and transmission matrices, $\mathbf{R}_T$ and $\mathbf{T}_T$ are given by

$$\begin{aligned} \mathbf{R}_T &= -\mathcal{T}_{22}^{-1}\mathcal{T}_{21} \\ \mathbf{T}_T &= \mathcal{T}_{11} - \mathcal{T}_{12}\mathcal{T}_{22}^{-1}\mathcal{T}_{21} \end{aligned} \tag{3.9a, b}$$

From an analytical viewpoint, equation (3.9) is identical to equation (3.3). The difference comes, however, from the formulation in describing wave motion. Compared to the method using reflection, transmission and propagation matrices, the transfer matrix method is convenient since the transfer matrix can be constructed by cascading matrices. However, as described in Appendix B, the transfer matrix method is not suitable in some situations.

3.3 Axial motion in a bar

Assume that the structure shown in Figure 12 is a bar undergoing axial vibration. For the bar, the reflection and transmission matrices are given by equation (2.38) and the propagation matrix between two junctions is defined by

$$\mathbf{F} = \left[\mathrm{e}^{-\mathrm{i}k_j L}\right] \tag{3.10}$$

3.3.1 Comparison of the two methods

Figure 13 shows the comparison of the power reflection and transmission coefficients obtained using the two numerical methods when the area changes are $A_2 = 2A_1$, $A_3 = 4A_1$. The two results are identical. This indicates that either method can be used for the analysis of axial

vibration.

3.3.2 *Effect of cross-section change ratio*

Figure 14 shows the power reflection and transmission coefficients when the area changes are $A_2 = 2A_1, A_3 = A_1$. Compared with Figure 13, it can be seen that the frequencies where the maximum and minimum transmission occur are reversed. The power transmission coefficient τ from equations (3.3) or (3.9) can be written as

$$\tau = \frac{4\alpha_{31}}{(1+\alpha_{31})^2 \cos^2 k_l L + (\alpha_{21}+\alpha_{32})^2 \sin^2 k_l L} \tag{3.11}$$

where $\alpha_{31} = A_3/A_1$, $\alpha_{21} = A_2/A_1$ and $\alpha_{32} = A_3/A_2$ represent the ratios of the cross-sectional areas. From equation (3.11), it can be shown that the maximum or minimum transmission occurs when $k_l L = \pi/2, \pi, 3\pi/2, \ldots$ and the maximum/minimum position is determined by the sign of $(1-\alpha_{21})(1-\alpha_{32})$. For example, when the cross-sectional areas increase monotonically, namely, $A_1 < A_2 < A_3$, the maximum transmission occurs when $k_l L = \pi/2, 3\pi/2, 5\pi/2, \ldots$ and the minimum transmission occurs when $k_l L = \pi, 2\pi, 3\pi, \ldots$.

It is clear that the reflection and transmission will be independent of the intermediate cross-sectional area A_2 if $k_l L$ is small. This explains why, in Figure 14, the transmission coefficient tends to unity as $k_l L$ tends to zero. It can also be noted that the transmission will be unity if $\sin k_l L = \pm 1$ and the intermediate cross-sectional area A_2 satisfies $A_2^2 = A_1 A_3$.

Figure 15 shows the power transmission coefficients when the cross-sectional area of the middle section varies. It can be seen that the greater the area change ratio becomes, the lower transmission efficiency.

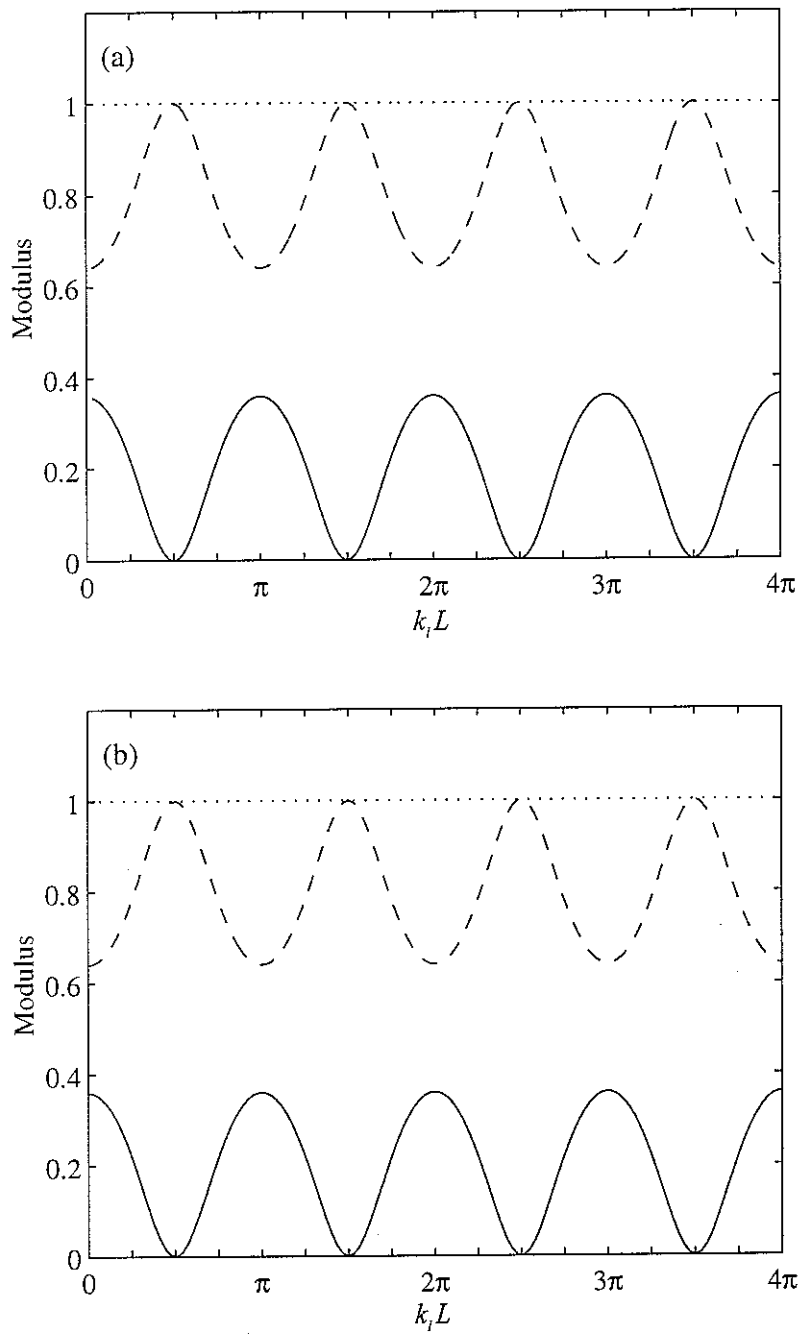

Figure 13. Power reflection/transmission coefficients for two area changes, $A \to 2A \to 4A$.

(a) Using reflection, transmission and propagation matrices, (b) using transfer matrix method.

——— , Reflection; ------ ,transmission; ..... , total power.

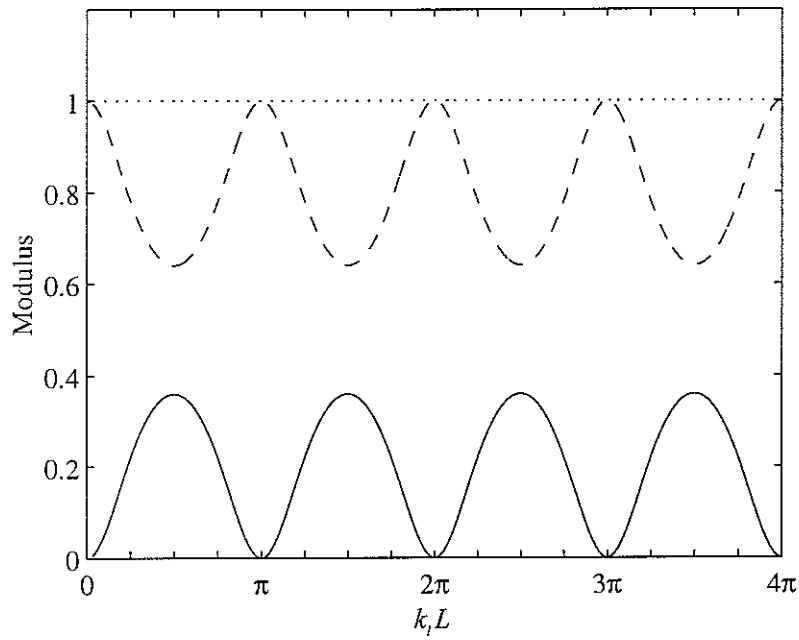

Figure 14. Power reflection/transmission coefficients for two area changes, $A \to 2A \to A$.

——— , Reflection; ------ , transmission; ..... , total power.

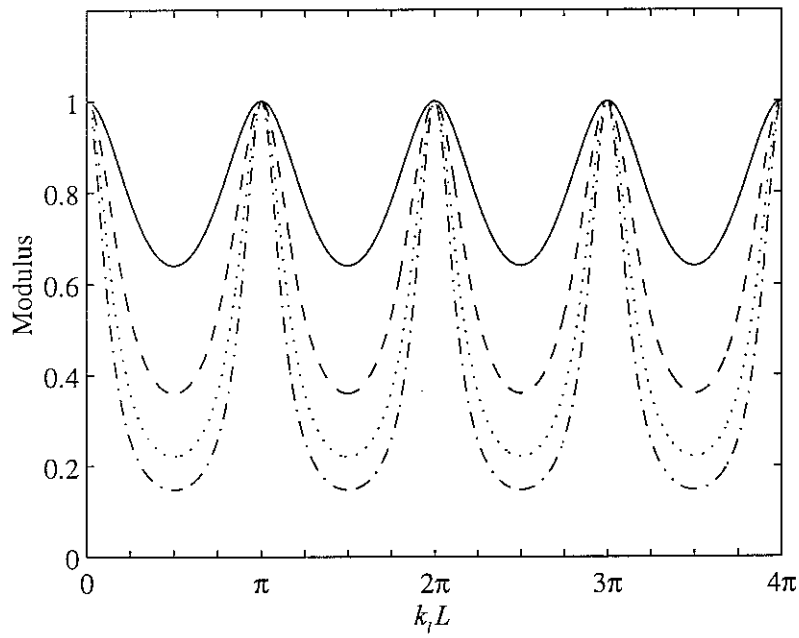

Figure 15. Effect of the cross-sectional area change ratio on the power transmission coefficients.

———, $A \to 2A \to A$; ------, $A \to 3A \to A$; ....., $A \to 4A \to A$; -·-·-·-, $A \to 5A \to A$.

3.4 Bending motion in a beam

Assume that the infinite structure shown in Figure 12 is a rectangular beam undergoing bending motion. For the beam, the reflection and transmission matrices are given by equation (2.47) and the propagation matrix between the two junctions is given by

$$\mathbf{F}=\begin{bmatrix} e^{-ik_{b,2}L} & 0 \\ 0 & e^{-k_{b,2}L} \end{bmatrix} \tag{3.12}$$

where the subscript 2 refers to the intermediate region and $k_{b,2}$ is the wavenumber in the intermediate region as shown in Figure 16.

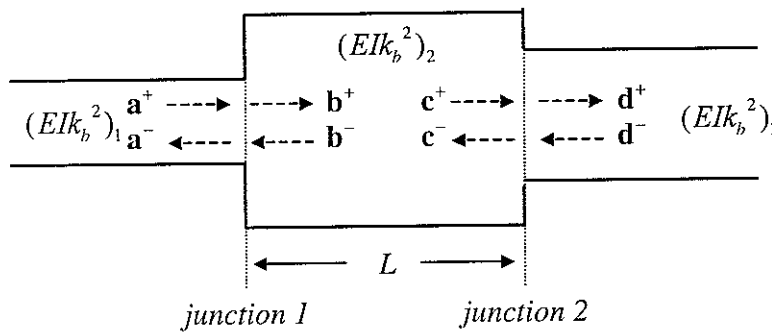

Figure 16. An infinite beam with two changes in cross-sectional area.

3.4.1 Effect of nearfield wave

Figures 17 to 19 show the net reflection and transmission coefficients for three typical cases where only the thickness h changes while the width b is constant. First, it can be seen that there are the coefficients for propagating waves generated by incident nearfield waves, namely, $T_{T,12}$ (element (1,2) of $\mathbf{T}_T$) and $R_{T,12}$ (element (1,2) of $\mathbf{R}_T$), which are not small compared to $T_{T,11}$ and $R_{T,11}$. This means that substantial propagating waves can be set up in region 3 by incident nearfield waves in region 1. Second, it can be seen that the value of k_bL for

the first maximum of transmission is larger than π. This is due to the influence of the nearfield waves in the intermediate region as described in Appendix A. This demonstrates that nearfield waves cannot be neglected if $k_b L$ is smaller than π.

The coefficient $T_{T,11}$ tends to unity when $k_b L$ tends to zero in Figure 17 and Figure 18. As noted in section 3.3.2, this indicates that the net reflection and transmission coefficients are independent of the intermediate cross-sectional area if $k_b L$ is small.

3.4.2 Comparison of the two numerical methods

Power reflection and transmission coefficients are investigated when only a propagating wave is incident on the first junction. Figure 20 shows results obtained by the two methods, one using reflection, transmission and propagation matrices and the other using the transfer matrix approach, when thickness of the beam changes from $h \rightarrow 1.1h \rightarrow h$. It can be seen that the second approach fails to give a reasonable result when $k_b L$ becomes large. As described in Appendix B, this is one of the numerical difficulties of the transfer matrix method because of the badly conditioned propagation matrix.

Figure 21 shows the power reflection and transmission coefficients obtained by the transfer matrix method when the thickness change is greater, namely $h \rightarrow 2h \rightarrow h$. It can be seen that numerical errors occur at a lower value of $k_b L$ compared with Figure 20-(b). Thus the lowest frequency below which the transfer matrix method is applicable is also dependent on the severity of non-uniformity of a beam, as well as the length compared to a wavelength.

3.4.3 Effect of cross-section change ratio

Figures 22 shows the power transmission coefficients for various width changes. As noted in section 2.5.2, the phases of the reflection and transmission coefficients are constant if the

thickness is constant and only the width changes. This explains why the maximum and minimum points of the power transmission do not change in Figure 22.

Figures 23 shows the power transmission coefficients for various thickness changes. It can be seen that the maximum and minimum points of the power transmission depends on the specific thickness changes and tend to a limit when the ratio of the thickness change becomes greater. The tendency can be understood by the fact that, as noted in section 2.5.2, the phase of the reflection coefficient R_{11} tends to $-\pi/2$ as the thickness difference increases.

As shown in Figure 24, Figure 23 can also be replotted as a function of the wavenumber $k_{b,1}$ of the first section of the beam. Figure 24 is more meaningful if the issue of most concern is in what frequency ranges substantial reflection and transmission occur.

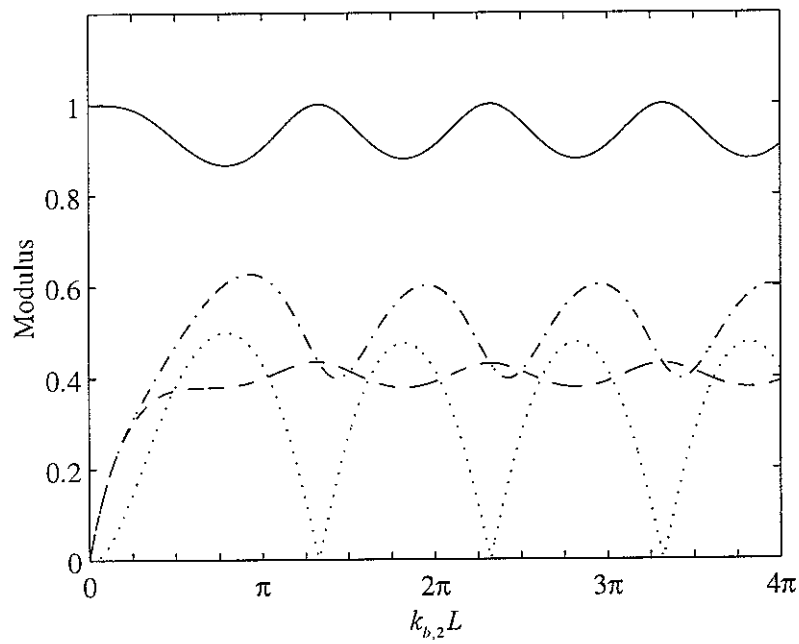

Figure 17. Reflection and transmission coefficients for thickness changes, $h \to 2h \to h$.

——— , $T_{T,11}$; ------ , $T_{T,12}$; ····· , $R_{T,11}$; -·-·-· , $R_{T,12}$.

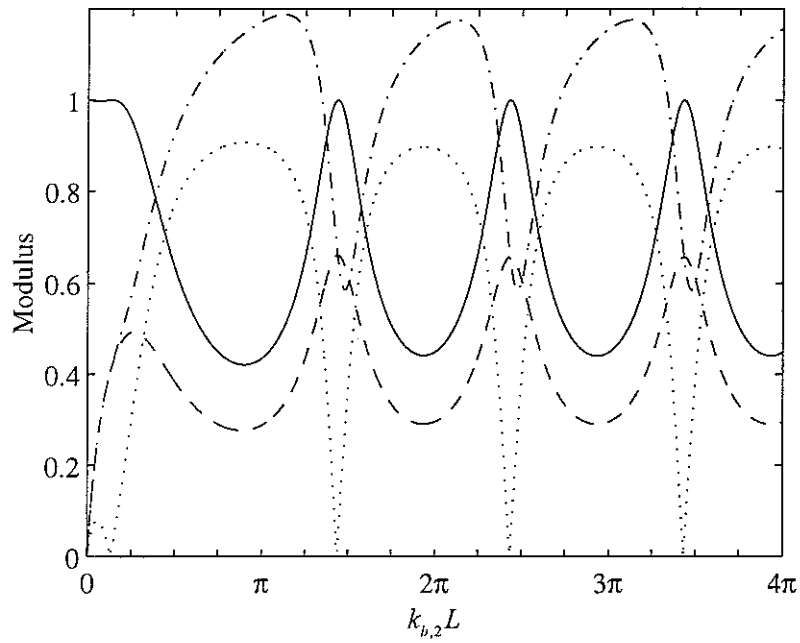

Figure 18. Reflection and transmission coefficients for thickness changes, $h \to 4h \to h$.

....., $T_{T,11}$; - - - - - -, $T_{T,12}$; ....., $R_{T,11}$; -.-.-.-, $R_{T,12}$.

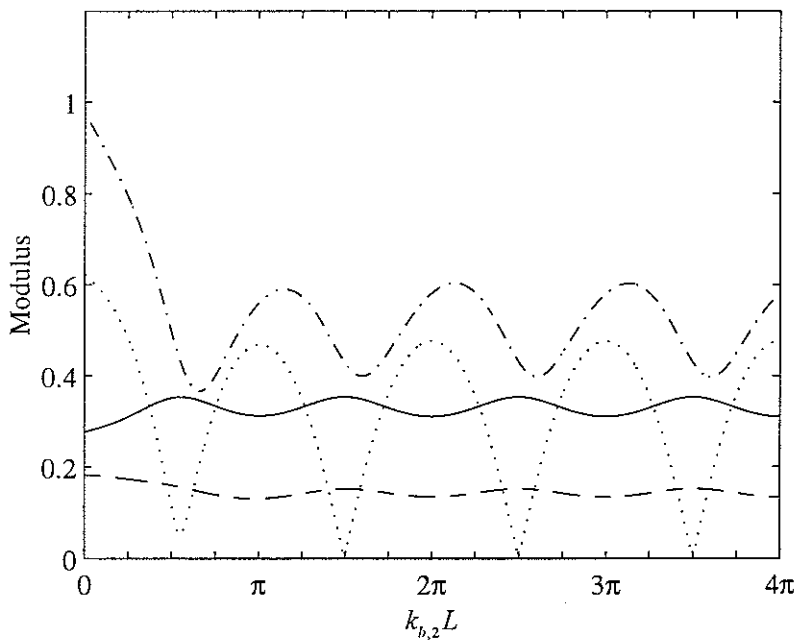

Figure 19. Reflection and transmission coefficients for thickness changes, $h \to 2h \to 4h$.

——, $T_{T,11}$; - - - - - -, $T_{T,12}$; ....., $R_{T,11}$; -.-.-.-, $R_{T,12}$.

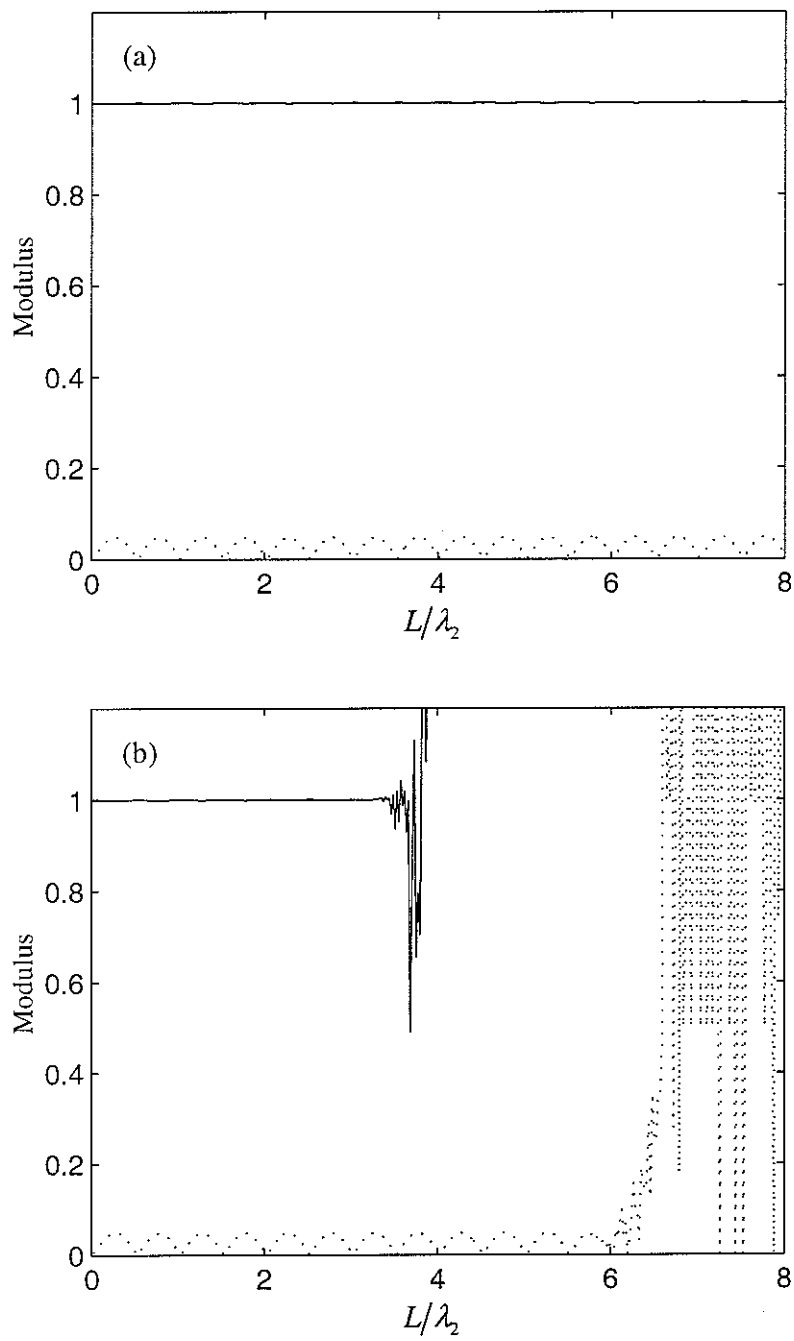

Figure 20. Reflection and transmission coefficients for thickness changes, $h \rightarrow 1.1h \rightarrow h$.

(a) Using reflection, transmission and propagation matrices, (b) using transfer matrix method.

——— , $T_{T,11}$; ····· , $R_{T,11}$.

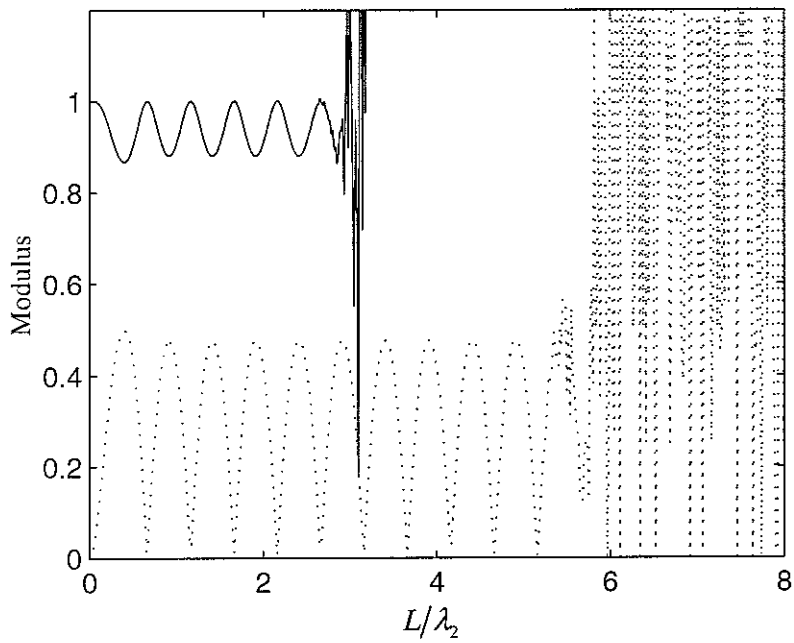

Figure 21. Reflection and transmission coefficients for thickness changes, $h \to 2h \to h$, obtained by transfer matrix method. ——— , $T_{T,11}$; ····· , $R_{T,11}$.

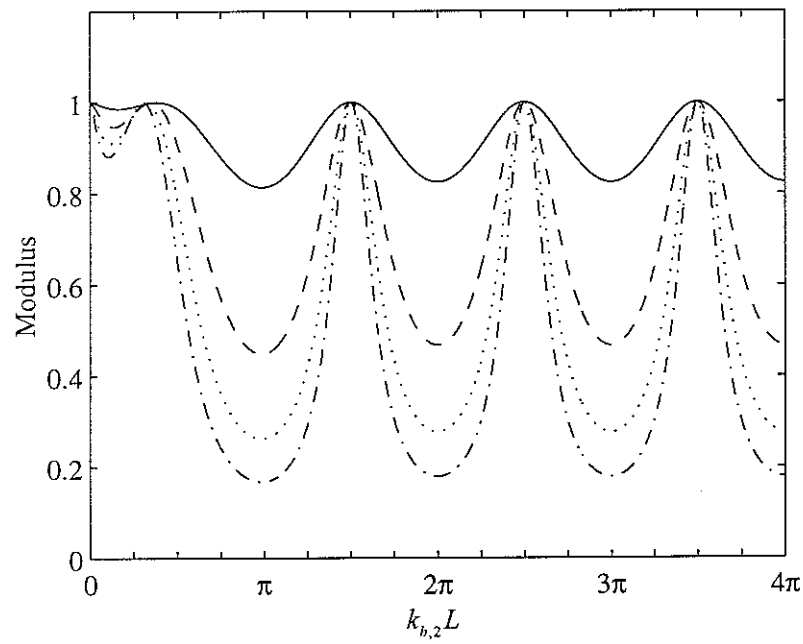

Figure 22. Power transmission coefficients for width changes. ——— , $b \to 4b \to b$; ------ , $b \to 8b \to b$; ····· , $b \to 12b \to b$; -·-·-·- , $b \to 16b \to b$.

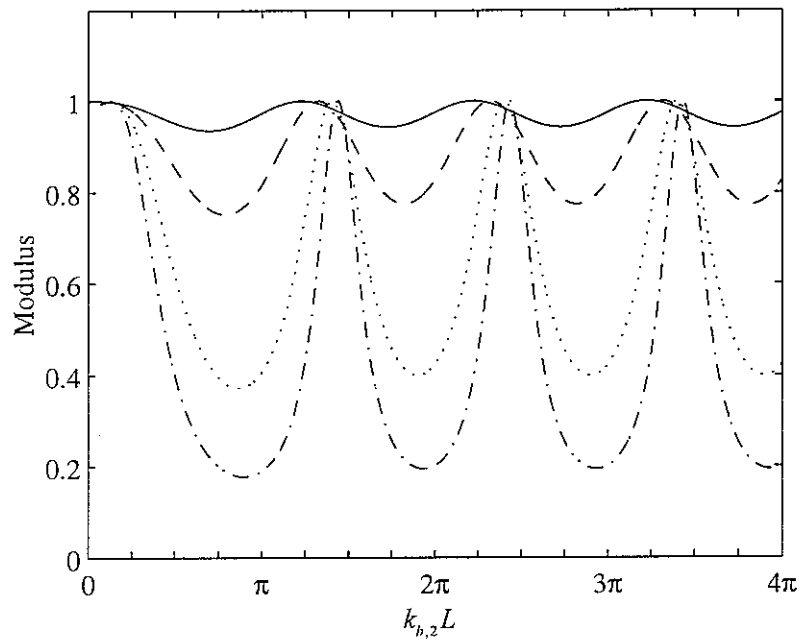

Figure 23. Power transmission coefficients for thickness changes. ——— , $h \to 1.5h \to h$; ------ , $h \to 2h \to h$; ..... , $h \to 3h \to h$; -.-.-.- , $h \to 4h \to h$.

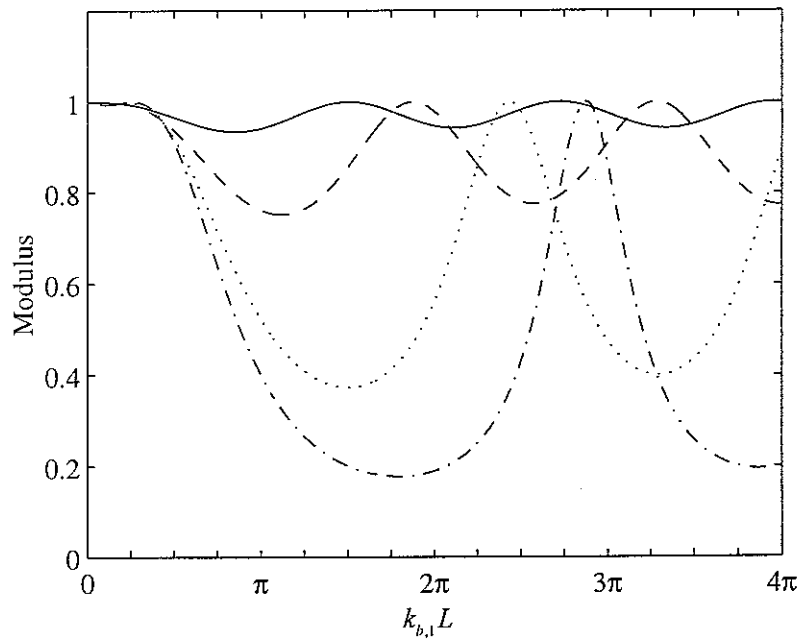

Figure 24. Power transmission coefficients for thickness changes as a function of $k_{b,1}$. ——— , $h \to 1.5h \to h$; ------ , $h \to 2h \to h$; ..... , $h \to 3h \to h$; -.-.-.- , $h \to 4h \to h$.

3.5 Summary

In this section, the net reflection and transmission for an infinite bar or beam with two changes in cross-sectional area in a region has been considered. The analysis has been performed using two different methods - the wave method using reflection, transmission and propagation matrices and the transfer matrix method. It was shown that, when nearfield waves exist, the transfer matrix method cannot be applied in the high frequency region. Thus this method can be used for axial vibration, but care must be taken when using this method for bending vibration.

In general, as the non-uniformity becomes severe, the more the incident waves are reflected. However, it should be noted that substantial propagating waves can be generated when nearfield waves are incident.

It has been shown that wave transmission and reflection for both a bar and a beam depend on the area changes. This implies that the pass-band and stop-band frequency ranges can be controlled by the design of the area variation in the structure.

It has also been shown that the thickness variation ratio can be another factor for vibration control in bending motion. The pass-band and stop-band frequency ranges will change according to the specific values of the thickness, which cannot be seen in the case of a bar or in the case of width change in a beam.

4. Continuously non-uniform structures

4.1 Introduction

In a structure with continuously varying non-uniformity, travelling waves are also continuously reflected and transmitted. However, if the structure is considered to be composed of many small sections with uniform properties, the vibration of the structure can be analysed with the discrete wave model described in section 3.

Similar to Finite Element Analysis, it may be supposed that the more sections are used, the more accurate are the predictions. In particular, it might be thought that the largest section length should be much shorter than the relevant wavelength. However, in the wave model, the determination of the section length is also related to the non-uniformity of the structure. For example, the wave model does not require the structure to be divided into small sections if the structure is uniform or the non-uniformity is very small. In section 4.2, this problem is discussed.

To illustrate the numerical errors that can occur in the wave method, the reflection and transmission of a conical connector in an infinite bar are investigated in section 4.3.

In section 4.4, the axial motion of a finite bar with conically varying radius is investigated. The results predicted using the wave method are compared with analytical calculations.

4.2 Numerical considerations

Consider the case where there is an infinite structure with continuously varying non-uniformity in a finite region of length L as shown in Figure 25. The discrete wave model can be applied on the assumption that the varying region consists of many small uniform sections. To identify the numerical errors due to the discretization, here, only one uniform section of length

Δx is considered to represent the variation.

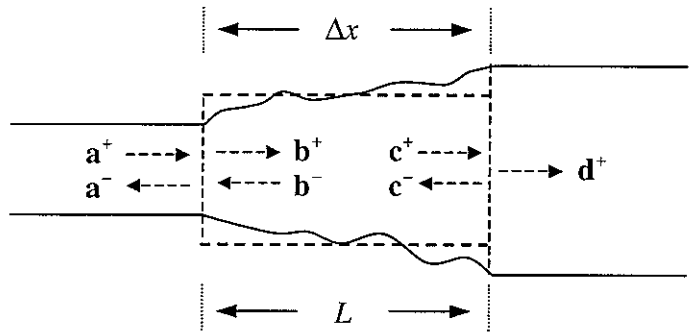

Figure 25. Infinite structure with continuously varying cross section in a finite region.

Recalling the discrete wave model described in section 3, the wave amplitudes vector $\mathbf{b}^+$ is given by

$$\mathbf{b}^+ = [\mathbf{I} - \hat{\mathbf{R}}_1 \mathbf{F} \mathbf{R}_2 \mathbf{F}]^{-1} \mathbf{T}_1 \mathbf{a}^+ \tag{4.1}$$

where the subscripts 1 and 2 refer to the left-hand and right-hand junctions of the varying region, respectively. As described in Appendix A, if the term $[\mathbf{I} - \hat{\mathbf{R}}_1 \mathbf{F} \mathbf{R}_2 \mathbf{F}]^{-1}$ is expanded as a power series, equation (4.1) can be written as

$$\mathbf{b}^+ = [\mathbf{I} + (\hat{\mathbf{R}}_1 \mathbf{F} \mathbf{R}_2 \mathbf{F}) + (\hat{\mathbf{R}}_1 \mathbf{F} \mathbf{R}_2 \mathbf{F})^2 + \ldots] \mathbf{T}_1 \mathbf{a}^+ \tag{4.2}$$

For simplicity, assuming that the reflection and transmission matrices are all scalars and the propagation matrix is given by $e^{-ik\Delta x}$, then equation (4.2) reduces to

$$\mathrm{b}^+ = [1 + \hat{R}_1 R_2 e^{-ik\,2\Delta x} + (\hat{R}_1 R_2)^2 e^{-ik\,4\Delta x} + \ldots] T_1 \mathrm{a}^+ \tag{4.3}$$

In the case where the structure is uniform, namely, $\hat{R}_1 R_2 = 0$ and $T_1 = 1$, the wave amplitude b^+ becomes

$$\mathrm{b}^+ = \mathrm{a}^+ \tag{4.4}$$

Equation (4.4) shows that it does not matter how the non-uniform region is divided when the structure is uniform.

In the non-uniform structure, the effect of the above terms from the third in the bracket in equation (4.3) can be neglected since $\hat{R}_1 R_2 < 1$. At this time, to avoid the aliasing effect, it is required that

$$2k\Delta x < \pi \tag{4.5}$$

Therefore the maximum wavenumber $k_{\max}$ is constrained by

$$k_{\max} < \frac{\pi}{2\Delta x} \tag{4.6}$$

In other words, the length Δx of the discrete uniform section should be smaller than the relevant wavelength , namely,

$$\Delta x < \frac{\lambda_{\min}}{4} \tag{4.7}$$

Equation (4.7) shows that the non-uniformity of the structure should be considered when the length of the section is determined.

It should be noted that equation (4.7) can be applied only for the propagating wave. The analysis for the case when nearfield waves exist is considered later.

4.3 Transmission through a conical connector

Consider the case where two semi-infinite cylindrical bars are connected by a bar having conically varying cross-sectional radius as shown in Figure 26. The radius r and the cross-sectional area A of the connector are given by

$$r = r_0\left(1+\alpha\frac{x}{L}\right), \quad A = A_0\left(1+\alpha\frac{x}{L}\right)^2 \tag{4.8a, b}$$

where r_0 is the initial radius, L is the length of the conical connector, α is a dimensionless parameter related to the taper rate and $A_0 = \pi r_0^2$ is the initial cross-sectional area.

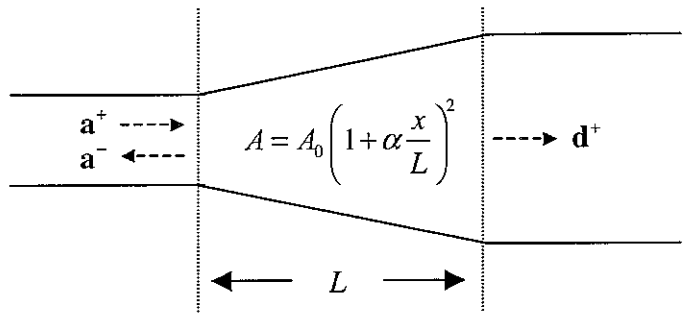

Figure 26. Infinite bar with a conical connector

If the transfer matrix method is applied to this case, the transmitted wave amplitude vector $\mathbf{d}^+$ can be written as

$$\begin{Bmatrix} \mathbf{d}^+ \\ \mathbf{0} \end{Bmatrix} = {}_d\mathcal{T}_a \begin{Bmatrix} \mathbf{a}^+ \\ \mathbf{a}^- \end{Bmatrix} \tag{4.9}$$

where ${}_d\mathcal{T}_a$ refers to transfer matrix for the conical connector. If the connector is considered to be composed of n uniform sections as shown in Figure 27, the transfer matrix ${}_d\mathcal{T}_a$ is given by

$${}_d\mathcal{T}_a = \mathcal{G}_{n+1}\mathcal{F}_n\mathcal{G}_n \ldots \mathcal{F}_1\mathcal{G}_1 \tag{4.10}$$

where $\mathcal{F}_1, \ldots, \mathcal{F}_n$ are the field transfer matrices of each section and $\mathcal{G}_1, \ldots, \mathcal{G}_n, \mathcal{G}_{n+1}$ are the point transfer matrices of each junction between sections.

Assume that all sections have the same length Δx and consider two discretization cases - namely the case where the conical connector is divided into two sections and the case where the connector is divided into 10 sections. The section lengths Δx are given by

$$\Delta x = \frac{L}{2}, \qquad \text{for } n = 2 \tag{4.11}$$

and

$$\Delta x = \frac{L}{10}, \qquad \text{for } n = 10 \tag{4.12}$$

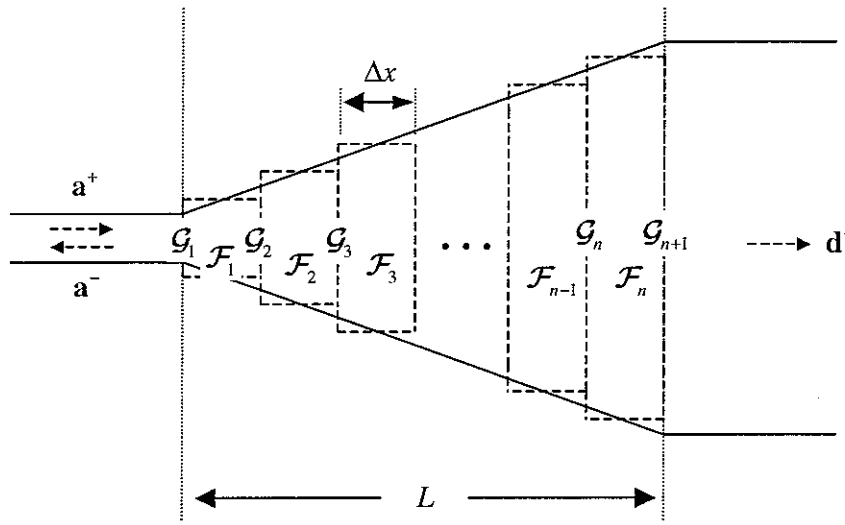

Figure 27. Discretization of a conical connector into small sections of constant length.

Therefore, according to equation (4.6), the maximum wavenumber $k_{l,\max}$ is given by

$$k_{l,\max} < \frac{\pi}{L}, \qquad \text{for } n = 2 \tag{4.13}$$

and

$$k_{l,\max} < \frac{5\pi}{L}, \qquad \text{for } n = 10 \tag{4.14}$$

Figure 28 shows the predicted power transmission coefficients for two discretization cases when $\alpha = 5$. Also, the numerical results are compared with the analytical solution which is described in detail in Appendix C. In Figure 28, it can be seen that, as the length Δx becomes smaller (namely, the more sections are considered), better results can be obtained. It can also be seen that, for the case when the connector is divided into 2 sections, the numerical errors become significant when $k_l > \pi/L$.

Figure 29 shows the predicted power transmission coefficients for two different values of the taper rate α. It can be seen that, as the taper rate α becomes greater, the numerical results become less accurate.

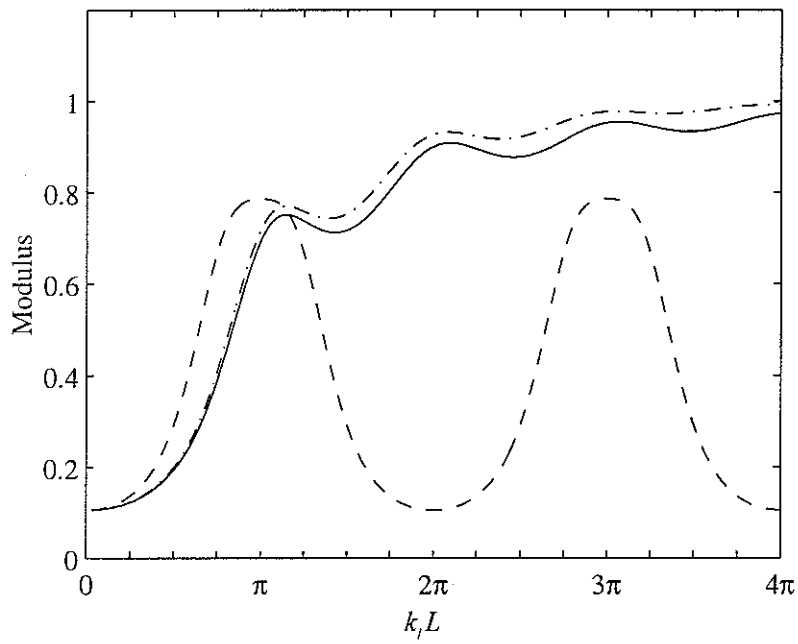

Figure 28. Power transmission coefficients for a conical connector.

——— , *analytical*; ------ , $\Delta x = L/2$; ·-·-·- , $\Delta x = L/10$.

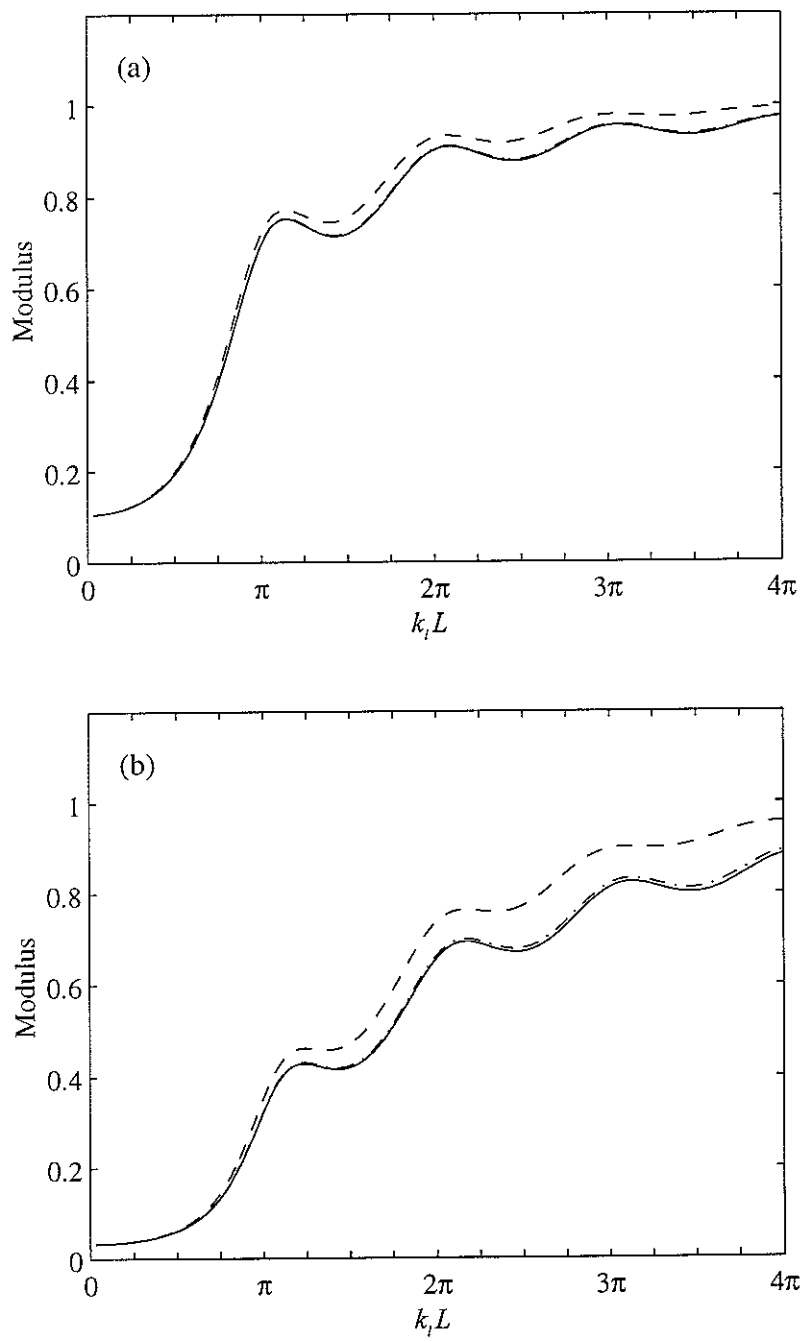

Figure 29. Power transmission coefficients for a conical connector. (a) $\alpha = 5$, (b) $\alpha = 10$.

——— , *analytical*; ------ , $\Delta x = L/10$; ------- , $\Delta x = L/40$.

4.4 Axial motion in a finite conical bar

Consider a finite bar with free-clamped ends as shown in Figure 30. It is assumed that the radius r and cross-sectional area A vary as given by equation (4.8) and a harmonic force, $Fe^{i\omega t}$ is applied at the free end.

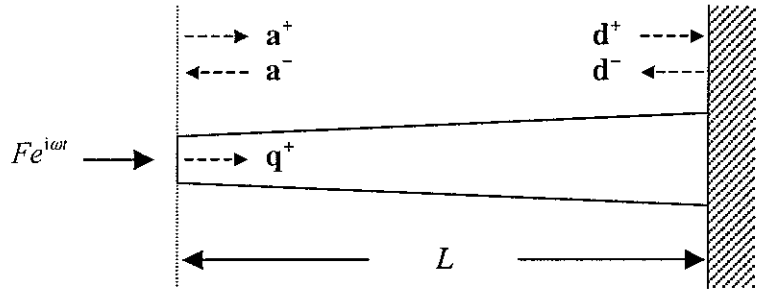

Figure 30. Finite bar with conical cross-sectional area change.

If the transfer matrix method is applied to this case, wave amplitude vectors $\mathbf{d}^+$ and $\mathbf{d}^-$ at the clamped end are given by

$$\begin{Bmatrix} \mathbf{d}^+ \\ \mathbf{d}^- \end{Bmatrix} = {}_d\mathcal{T}_a \begin{Bmatrix} \mathbf{a}^+ \\ \mathbf{a}^- \end{Bmatrix} \tag{4.15}$$

where $\mathbf{a}^+$ and $\mathbf{a}^-$ are the wave amplitude vectors at the free end and ${}_d\mathcal{T}_a$ is the transfer matrix from the free end to the clamped end. If the bar is assumed to be composed of n uniform sections, the transfer matrix ${}_d\mathcal{T}_a$ is given by

$${}_d\mathcal{T}_a = \mathcal{F}_n \mathcal{G}_{n-1} \mathcal{F}_{n-1} \cdots \mathcal{G}_1 \mathcal{F}_1 \tag{4.16}$$

where $\mathcal{F}_1, \ldots, \mathcal{F}_n$ are the field transfer matrices of each section and $\mathcal{G}_1, \ldots, \mathcal{G}_{n-1}$ are the point transfer matrices of each junction between sections. The boundary conditions are given by

$$\mathbf{a}^+ = \mathbf{R}_a \mathbf{a}^- + \mathbf{q}^+, \qquad \mathbf{d}^- = \mathbf{R}_d \mathbf{d}^+ \tag{4.17a, b}$$

where $\mathbf{R}_a$ and $\mathbf{R}_d$ are the reflection matrices of the boundaries and $\mathbf{q}^+$ is the vector of the forced wave amplitudes. Equations from (4.15) to (4.17) are general forms which can be applied to any kind of finite structure including bending motion of a beam. In this case, the boundary reflection matrices $\mathbf{R}_a$ and $\mathbf{R}_d$ are given by

$$\mathbf{R}_a = 1, \qquad \mathbf{R}_d = -1 \tag{4.18a, b}$$

and the forcing wave $\mathbf{q}^+$ is given by

$$\mathbf{q}^+ = -\mathrm{i}\frac{F}{EAk_l} \tag{4.19}$$

From equations from (4.15) to (4.19), the wave amplitude vectors $\mathbf{a}^+$ and $\mathbf{a}^-$ can be calculated and therefore, the receptance at the driving point can be obtained by

$$\frac{u}{F} = \frac{1}{F}\left(\mathbf{a}^+ + \mathbf{a}^-\right) \tag{4.20}$$

Figure 31 shows the predicted amplitudes of the receptances at the driving point for three different bars - namely, a uniform bar having no area change ($r = 1.5r_0$), a bar with gradually increasing area change ($r_0 \rightarrow 2r_0, \alpha = 1$) and a bar with gradually decreasing area change ($2r_0 \rightarrow r_0$, $\alpha = -0.5$). In this case, it is assumed that the bars are divided into 100 sections and all sections have same length $\Delta x = L/100$.

First of all, it can be seen that the resonances of the uniform bar occur when $k_l L$ is an odd multiple of $\pi/2$. It can also be seen that the resonances of the bar with $\alpha = 1$ occur when $k_l L$ is higher than an odd multiple of $\pi/2$ but the resonances of the bar with $\alpha = -0.5$ occur when $k_l L$ is lower than an odd multiple of $\pi/2$.

It can also be seen that the values of $k_l L$ of the three bars are significantly different for lower modes but become much closer to an odd multiple of $\pi/2$ for higher modes.

These predicted results are in good agreement with the analytical analysis described in appendix C.

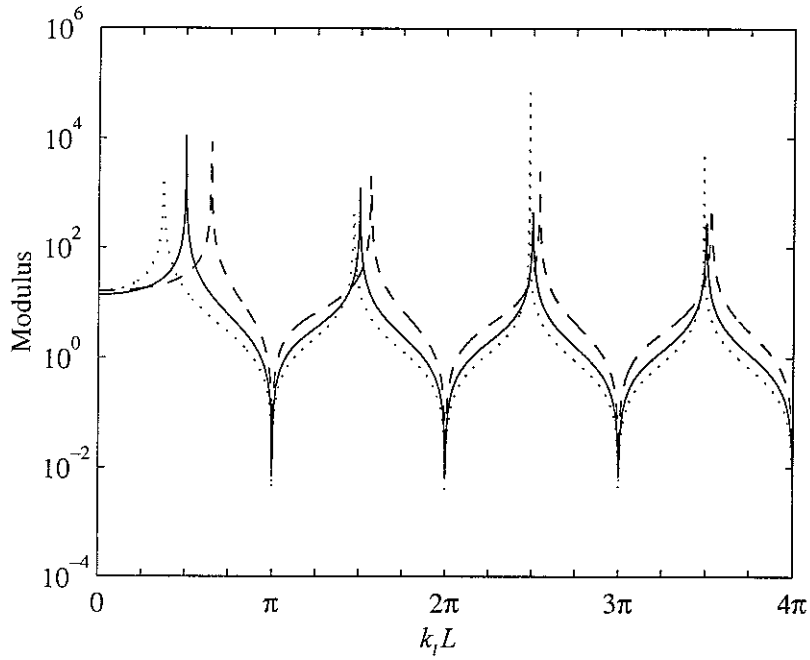

Figure 31. Receptances at driving point of three different bars. ——— , Uniform bar; ------ , gradually increasing conical bar ($\alpha = 1$); ····· , gradually decreasing conical bar ($\alpha = -0.5$).

4.5 Summary

In this section, it has been shown how the wave approach can be applied to a continuously non-uniform structure. If the structure is assumed to be composed of many uniform sections, the discrete wave model can be applied.

In section 4.2 and 4.3, the numerical errors due to the discretization of the continuous structure were considered. It was shown that the largest section length Δx is also related to the non-uniformity of the structure and largest section length Δx should be shorter than the relevant wavelength λ, roughly, $\Delta x < \frac{\lambda_{\min}}{4}$. Thus the more sections should be used for a structure with severe non-uniformity.

In section 4.4, the axial motion of a conical bar was investigated. It was shown that the

results predicted by the wave method show good agreement with the analytical solution. It was also seen that the natural frequencies of lower natural modes are much more affected by non-uniformities but the natural frequencies of higher modes are less affected. However, it should be noted that the small change of natural frequency due to non-uniformity does not imply a small change in the mode shape.

5. Conclusions

In this report, wave methods have been developed for the analysis of the vibration of a non-uniform one-dimensional structure. Although the work is mainly concerned with the axial vibration in a bar and the bending motion in a beam, the methods developed here could be applied to other structures.

In section 2, general wave theory for bars and beams was reviewed. The wave formulation for the deflections and internal forces was introduced. The reflection, transmission and propagation of the waves were investigated for various conditions and defined in matrix form.

In section 3, wave approach methods were applied to a structure which has discretely varying non-uniformity. Two approaches were developed. One is the method using reflection, transmission and propagation matrices and the other is the transfer matrix method. It was shown that, in the presence of nearfield waves, the transfer matrix method could not be applied in the high frequency region due to numerical errors. Another numerical difficulty of the transfer matrix method, as described in Appendix B, may occur when the transmission matrix is singular or nearly singular.

The concept of vibration control or confinement using non-uniformity has been briefly investigated. The results show the possibility that pass-band and stop-band frequency ranges could be controlled by the non-uniformity of the structure without adding external elements.

In section 4, the wave approach methods were applied to a structure which has continuously varying non-uniformity. It was shown that the discrete wave methods could be applied to the continuous non-uniform structure. However, care must be taken in dividing the structure into smaller uniform sections. The section size, which is required to avoid the numerical

errors due to the discretization, is related to the relevant wavelength and the severity of the non-uniformity.

The transmission through a conical connector and the behaviour of a finite conical bar were also investigated. The numerical results showed good agreement with the analytical calculations.

Appendix A. Influence of nearfield waves

As a simple example to illustrate the influence of nearfield waves, consider an infinite uniform beam with two simple supports as shown in Figure A-1. For simplicity, it is assumed that the incident wave vector consists of a propagating wave and has no nearfield wave component, namely,

$$\mathbf{a}^{+} = \begin{Bmatrix} a^{+} \\ 0 \end{Bmatrix} \tag{A.1}$$

The reflection and transmission matrices, $\mathbf{R}$ and $\mathbf{T}$ of a simple support are given by equation (2.44) and the propagation matrix $\mathbf{F}$ from the left to the right support is given by

$$\mathbf{F} = \begin{bmatrix} e^{-ik_b L} & 0 \\ 0 & e^{-k_b L} \end{bmatrix} \tag{A.2}$$

Now, the relevant wave amplitude vectors in this case can be written as

$$\begin{aligned} \mathbf{b}^{+} &= \mathbf{T}\mathbf{a}^{+} + \mathbf{R}\mathbf{b}^{-} \\ \mathbf{c}^{+} &= \mathbf{F}\mathbf{b}^{+} \\ \mathbf{c}^{-} &= \mathbf{R}\mathbf{c}^{+} \\ \mathbf{b}^{-} &= \mathbf{F}\mathbf{c}^{-} \\ \mathbf{a}^{-} &= \mathbf{R}\mathbf{a}^{+} + \mathbf{T}\mathbf{b}^{-} \\ \mathbf{d}^{+} &= \mathbf{T}\mathbf{c}^{+} \end{aligned} \tag{A.3a, b, c, d, e, f}$$

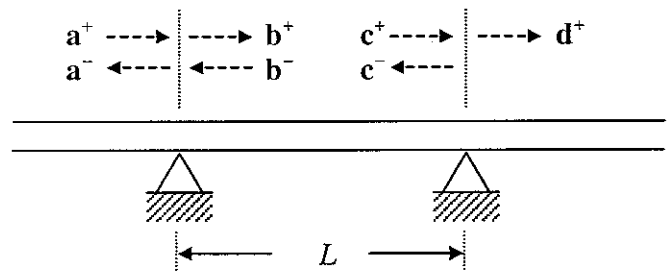

Figure A-1. Infinite beam with two simple supports.

Rearranging equation (A.3) in terms of the incident wave amplitude vector $\mathbf{a}^+$ yields

$$\begin{aligned}\mathbf{b}^+ &= [\mathbf{I}-\mathbf{RFRF}]^{-1}\mathbf{Ta}^+ \\ \mathbf{c}^+ &= \mathbf{F}[\mathbf{I}-\mathbf{RFRF}]^{-1}\mathbf{Ta}^+ \\ \mathbf{c}^- &= \mathbf{RF}[\mathbf{I}-\mathbf{RFRF}]^{-1}\mathbf{Ta}^+ \\ \mathbf{b}^- &= \mathbf{FRF}[\mathbf{I}-\mathbf{RFRF}]^{-1}\mathbf{Ta}^+\end{aligned} \qquad \text{(A.4a, b, c, d)}$$

and

$$\begin{aligned}\mathbf{a}^- &= \left(\mathbf{R}+\mathbf{TFRF}[\mathbf{I}-\mathbf{RFRF}]^{-1}\mathbf{T}\right)\mathbf{a}^+ \\ \mathbf{d}^+ &= \mathbf{TF}[\mathbf{I}-\mathbf{RFRF}]^{-1}\mathbf{Ta}^+\end{aligned} \qquad \text{(A.5a, b)}$$

In equation (A.5), the terms multiplying the incident wave amplitude vector $\mathbf{a}^+$ are the net reflection and transmission matrices, $\mathbf{R}_T$ and $\mathbf{T}_T$, through two simple supports, namely,

$$\begin{aligned}\mathbf{R}_T &= \begin{bmatrix} R_{T,11} & R_{T,12} \\ R_{T,21} & R_{T,22}\end{bmatrix} = \left(\mathbf{R}+\mathbf{TFRF}[\mathbf{I}-\mathbf{RFRF}]^{-1}\mathbf{T}\right) \\ \mathbf{T}_T &= \begin{bmatrix} T_{T,11} & T_{T,12} \\ T_{T,21} & T_{T,22}\end{bmatrix} = \mathbf{TF}[\mathbf{I}-\mathbf{RFRF}]^{-1}\mathbf{T}\end{aligned} \qquad \text{(A.6a, b)}$$

Since the incident wave vector has no nearfield wave component and the nearfield components in the reflected and transmitted waves do not carry energy, the power reflection and transmission coefficients, ϱ and τ, can be written as

$$\varrho = \left|R_{T,11}\right|^2, \qquad \tau = \left|T_{T,11}\right|^2 \qquad \text{(A.7a, b)}$$

Figure A-2 shows the power reflection and transmission coefficients. It can be seen that the influence of nearfield waves cannot be neglected if $k_b L < \pi$.

The term $[\mathbf{I}-\mathbf{RFRF}]^{-1}$ in equations (A.4) and (A.5) can be interpreted as follows. Using a power series expansion, it can be written as

$$[\mathbf{I}-\mathbf{RFRF}]^{-1} = \mathbf{I}+(\mathbf{RFRF})+(\mathbf{RFRF})^2+(\mathbf{RFRF})^3+\ldots \qquad \text{(A.8)}$$

In equation (A.8), each term represents the wave propagation around the circuit between the two simple supports. If the influence of nearfield waves can be neglected, the term **RFRF** reduces

to

$$\mathbf{RFRF} = \left(\frac{-1}{1-\mathrm{i}}\right)^2 e^{-\mathrm{i}2k_b L} = \frac{1}{2} e^{-\mathrm{i}(2k_b L - \pi/2)} \tag{A.9}$$

Equations (A.6) and (A.9) show that the maximum transmission will occur when the phase of the term **RFRF** is a multiple of 2π. Thus, if the influence of nearfield waves can be neglected, the maximum transmission occurs when

$$k_b L = \frac{(4n+1)\pi}{4} \tag{A.10}$$

where $n = 0, 1, 2, 3, \ldots$. The maximum value of the power transmission coefficient is given by

$$\tau_{\max} = 1 \tag{A.11}$$

since

$$[\mathbf{I} - \mathbf{RFRF}]^{-1} = 1 + \left(\frac{1}{2}\right) + \left(\frac{1}{2}\right)^2 + \left(\frac{1}{2}\right)^2 + \ldots = 2 \tag{A.12}$$

The minimum transmission occurs when

$$k_b L = \frac{(4n+3)\pi}{4} \tag{A.13}$$

and the minimum value of the power transmission coefficient is given by

$$\tau_{\min} = \frac{1}{9} \tag{A.14}$$

since

$$[\mathbf{I} - \mathbf{RFRF}]^{-1} = 1 - \left(\frac{1}{2}\right) + \left(\frac{1}{2}\right)^2 - \left(\frac{1}{2}\right)^3 + \ldots = \frac{2}{3} \tag{A.15}$$

Meanwhile, since no energy dissipation is assumed in this case, the maximum and minimum values of the power reflection coefficient can be easily determined using equation (2.60). These results show good agreement with Figure A-2.

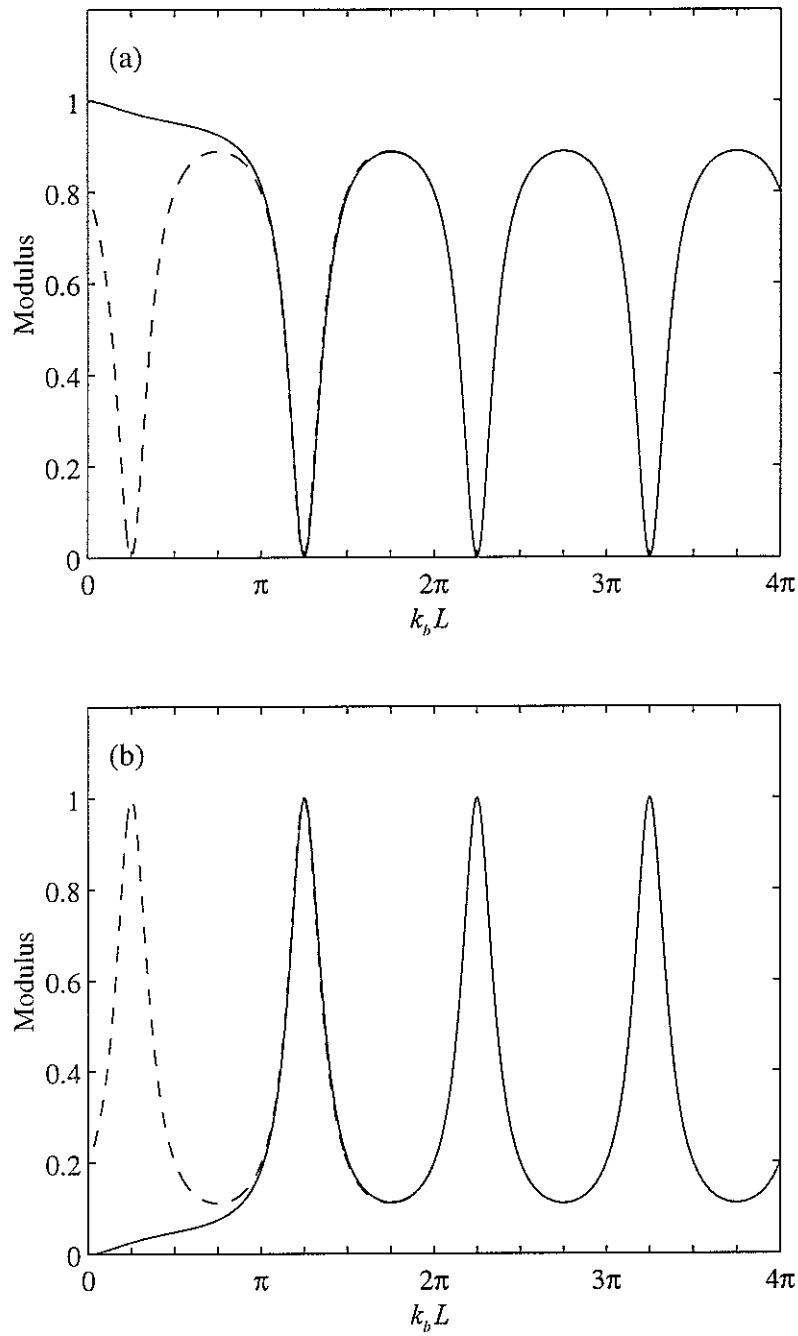

Figure A-2. Power reflection and transmission coefficients of two simply supported points in a beam. (a) Reflection coefficient, (b) transmission coefficient. ——— , Including nearfield wave components, ------ , excluding nearfield wave components.

Appendix B. Wave analysis by transfer matrix method

The transfer matrix defines the dynamic relationships of the element between two stations and allows the state vector for the deflections and internal forces to be transferred from one station to the next station [9]. Figure B-1 shows a drawing analogous to the Holzer-Myklestad model, in which each station represents a point (or localized) discontinuity.

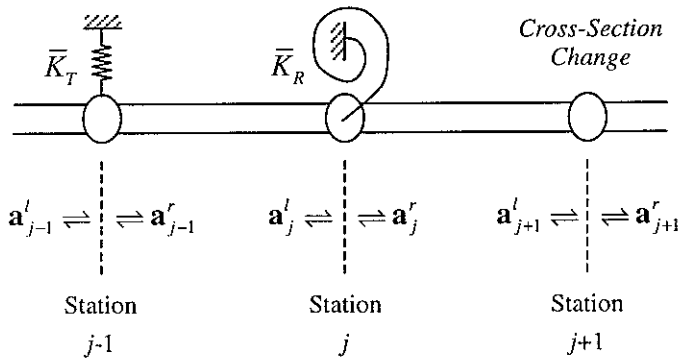

Figure B-1. Wave analysis by transfer matrix method.

If the wave amplitude vector $\mathbf{a}$ including positive-going and negative-going waves is introduced, the left-hand side wave amplitude vector $\mathbf{a}^l_j$ of a station j can be written as

$$\mathbf{a}^l_j = \begin{Bmatrix} \mathbf{a}^+ \\ \mathbf{a}^- \end{Bmatrix}^l_j \tag{B.1}$$

where $\mathbf{a}^+$ and $\mathbf{a}^-$ are the vectors of positive-going and negative-going wave amplitudes, respectively, and the superscript l and subscript j refer to the left-hand side of the station j. The left-hand side wave amplitude vector $\mathbf{a}^l_j$ of the station j can be expressed in terms of the

right-hand side wave amplitude vector $\mathbf{a}_{j-1}^{r}$ of the station $j-1$ as

$$\mathbf{a}_j^l = \mathcal{F}_j \mathbf{a}_{j-1}^r \tag{B.2}$$

In equation (B.2), the matrix $\mathcal{F}_j$ is called a field transfer matrix from station $j-1$ to station j and is given by

$$\mathcal{F}_j = \begin{bmatrix} \mathbf{F}_j & 0 \\ 0 & \mathbf{F}_j^{-1} \end{bmatrix} \tag{B.3}$$

where $\mathbf{F}_j$ is a propagation matrix from the station $j-1$ to the station j. Similarly, the right-hand wave amplitude vector $\mathbf{a}_j^r$ can be expressed in terms of the left-hand wave amplitude vector $\mathbf{a}_j^l$ as

$$\mathbf{a}_j^r = \mathcal{G}_j \mathbf{a}_j^l \tag{B.4}$$

In equation (B.4), the matrix $\mathcal{G}_j$ is a point transfer matrix and is given by

$$\mathcal{G}_j = \begin{bmatrix} \mathbf{T}_j - \hat{\mathbf{R}}_j \hat{\mathbf{T}}_j^{-1} \mathbf{R}_j & \hat{\mathbf{R}}_j \hat{\mathbf{T}}_j^{-1} \\ -\hat{\mathbf{T}}_j^{-1} \mathbf{R}_j & \hat{\mathbf{T}}_j^{-1} \end{bmatrix} \tag{B.5}$$

where $\mathbf{R}_j$ and $\mathbf{T}_j$ are the reflection and transmission matrices from the left-hand side to the right-hand side at the station j, respectively, and $\hat{\mathbf{R}}_j$ and $\hat{\mathbf{T}}_j$ are the reflection and transmission matrices from the right-hand side to the left-hand side at the station j, respectively. Successively applying equations (B.2) and (B.4) yields

$$\begin{aligned} \mathbf{a}_1^l &= \mathcal{F}_1 \mathbf{a}_0^r \\ \mathbf{a}_1^r &= \mathcal{G}_1 \mathcal{F}_1 \mathbf{a}_0^r \\ &\vdots \\ \mathbf{a}_j^r &= \mathcal{F}_j \mathcal{G}_{j-1} \mathcal{F}_{j-1} \cdots \mathcal{G}_1 \mathcal{F}_1 \mathbf{a}_0^r \end{aligned} \tag{B.6a, b, ..., c}$$

or more concisely

$$\mathbf{a}_j^l = {}_j^l\mathcal{T}_0^r \mathbf{a}_0^r \tag{B.7}$$

In equation (B.7), the matrix ${}_j^l\mathcal{T}_0^r$ is a transfer matrix that represents the dynamic relationships from the right-hand side of station 0 to the left-hand side of station j.

The boundary conditions can be considered after the transfer matrix for the whole structure is constructed. If the reflection matrices at the boundaries are given by $\mathbf{R}_{bj}$ and $\hat{\mathbf{R}}_{b0}$, then the wave amplitudes at the boundaries can be written as

$$\mathbf{a}_j^l = \begin{Bmatrix} \mathbf{a}^+ \\ \mathbf{R}_{bj}\mathbf{a}^+ \end{Bmatrix}_j^l, \qquad \mathbf{a}_0^r = \begin{Bmatrix} \hat{\mathbf{R}}_{b0}\mathbf{a}^- \\ \mathbf{a}^- \end{Bmatrix}_0^r \tag{B.8a, b}$$

With equations (B.8) and (B.7), the structure can be analyzed.

The transfer matrix method appears to be attractive because the whole transfer matrix can be easily constructed by simple multiplication.

However, there are two kinds of numerical difficulties that occur when using the transfer matrix method [12]. The first occurs when the transmission matrix is singular and its inverse matrix in equation (B.5) does not exist. In fact, the transmission matrix will always be singular if either one of the displacements or the internal forces is zero at the discontinuity. For example, if the stiffness of an intermediate elastic support is very large compared to the bending stiffness of the beam, numerical difficulties may arise.

The second difficulty is related to the field transfer matrix including the inverse of the propagation matrix, $\mathbf{F}^{-1}$ as shown in equation (B.3). If a wave decays along a structure, such as the nearfield wave in a beam, numerical problem may arise. For example, consider a beam with two impedance-mismatching components separated by length L. The inverse of propagation matrix, $\mathbf{F}^{-1}$, for the intermediate region of the length L in this case is given by

$$\mathbf{F}^{-1} = \begin{bmatrix} e^{ik_b L} & 0 \\ 0 & e^{k_b L} \end{bmatrix} \tag{B.9}$$

Since $e^{k_b L}$ increases logarithmically, the difference between $e^{ik_b L}$ and $e^{k_b L}$ will be greater as $k_b L$ increases. For example, when $L/\lambda = 6$ (or, $k_b L \approx 38$), the 2-norm condition number of $\mathbf{F}^{-1}$ is approximately 10^{16} [16]. This means that the round-off error in the computational process will be significant so that the numerical result will become inaccurate.

Appendix C. Analytical analysis of axial vibration of a conical bar

1. Exact solution of governing equation

Recalling the governing equation of a bar with varying cross-section for free vibration, the axial displacement $u(x,t)$ is governed by

$$\frac{\partial}{\partial x}\left[EA(x)\frac{\partial u}{\partial x}\right]=\rho A(x)\frac{\partial^2 u}{\partial t^2} \tag{C.1}$$

Equation (C.1) can be rewritten as [1]

$$\left\{\frac{\partial^2}{\partial x^2}+\frac{1}{4A^2}[(A')^2-2AA'']-\frac{\rho}{E}\frac{\partial^2}{\partial t^2}\right\}A^{1/2}u=0 \tag{C.2}$$

where the primes denote differentiation with respect to x. It can be easily solved for the case where the coefficient $(1/4A^2)[(A')^2-2AA'']$ is constant. If this constant is written as $-m^2$ and the cross-sectional area A is given by πr^2, an ordinary differential equation is obtained where,

$$\frac{d^2r(x)}{dx^2}=m^2r(x) \tag{C.3}$$

where $r(x)$ refers to the radius of the cylindrical bar as a function of x.

There are several bars whose radius satisfies equation (C.3). The case $m=0$ yields the solution

$$r=r_0\left(1+\alpha\frac{x}{L}\right) \tag{C.4}$$

where r_0 refers to the initial radius of the bar and α is a dimensionless parameter. This case describes a linearly tapered bar or a conical bar. The other types satisfying equation (C.3) are

- Exponential : $r=r_0e^{mx}$ $_{or}$ r_0e^{-mx}

- Catenoidal : $r=r_0\cosh mx$ $_{or}$ $r_0\sinh mx$

- Sinusoidal : $r = r_0 \sin mx$ $_{or}$ $r_0 \cos mx$

For a conical bar ($m = 0$), equation (C.2) reduces to

$$\frac{\partial^2 (A^{1/2} u)}{\partial x^2} = \frac{\rho}{E} \frac{\partial^2 (A^{1/2} u)}{\partial t^2} \tag{C.5}$$

and, if a new variable $v(x,t) = A^{1/2} u(x,t)$ is introduced, it can be written as

$$\frac{\partial^2 v}{\partial x^2} = \frac{\rho}{E} \frac{\partial^2 v}{\partial t^2} \tag{C.6}$$

This is the wave equation. Therefore, suppressing the time dependence, its solution is given by

$$v(x) = C_1 e^{-ik_l x} + C_2 e^{+ik_l x} \tag{C.7}$$

or the original displacement is given by

$$u(x) = \frac{1}{(1+\alpha x/L)} (C_1 e^{-ik_l x} + C_2 e^{+ik_l x}) \tag{C.8}$$

where C_1 and C_2 are arbitrary constants which are determined by boundary conditions. Equation (C.8) shows that the axial vibration of a conical bar can be expressed as the sum of a positive-going wave and a negative-going wave. It also shows that the amplitude of the displacement increases or decreases according to the sign of α as the wave propagates along x.

2. Reflection and transmission through a conical connector

Consider the case where two semi-infinite cylindrical bars are connected with a bar having conically varying cross-sectional area as shown in Figure C-1. If the displacement in the conical connector is given as equation (C.8), then continuity of displacement and equilibrium of axial force at the left- and right-end junctions, respectively, yields

$$\begin{aligned} (C_1 + C_2) &= \mathbf{a}^+ + \mathbf{a}^- \\ -\frac{\alpha}{L}(C_1 + C_2) + (-ik_l C_1 + ik_l C_2) &= -ik_l \mathbf{a}^+ + ik_l \mathbf{a}^- \end{aligned} \tag{C.9a, b}$$

$$\frac{1}{1+\alpha}\left(C_1 e^{-ik_l L}+C_2 e^{+ik_l L}\right)=\mathbf{d}^+$$

$$-\frac{\alpha}{L(1+\alpha)^2}\left(C_1 e^{-ik_l L}+C_2 e^{+ik_l L}\right)+\frac{1}{1+\alpha}\left(-ik_l C_1 e^{-ik_l L}+ik_l C_2 e^{+ik_l L}\right)=-ik_l\mathbf{d}^+ \qquad \text{(C.10a, b)}$$

where $\mathbf{a}^+$, $\mathbf{a}^-$ and $\mathbf{d}^+$ refer to the incident, reflected and transmitted wave amplitude vectors, respectively.

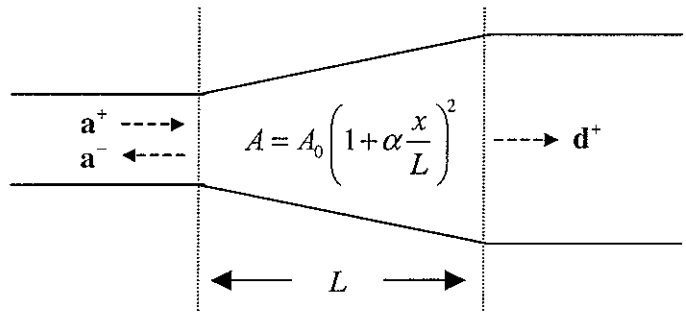

Figure C-1. Infinite bar with conical area change.

From equations (C.9) and (C.10), the transmitted wave amplitude vector $\mathbf{d}^+$ can be expressed in terms of the incident wave amplitude vector $\mathbf{a}^+$ by

$$\mathbf{d}^+ = e^{-ik_l L}\left[(1+\alpha)+\frac{\alpha^2}{4k_l^{\,2}L^2}\left\{1-i2k_l L-e^{-i2k_l L}\right\}\right]^{-1}\mathbf{a}^+ \qquad \text{(C.11)}$$

Therefore the power transmission coefficient is given by

$$\tau=(1+\alpha)^2\left|\frac{\mathbf{d}^+}{\mathbf{a}^+}\right|^2 \qquad \text{(C.12)}$$

When $k_l L\to 0$, the power transmission coefficient τ asymptotes to

$$\tau=\frac{4(1+\alpha)^2}{(2+2\alpha+\alpha^2)^2} \qquad \text{(C.13)}$$

and when $k_l L\to\infty$, asymptotes to

$$\tau=1 \qquad \text{(C.14)}$$

3. Natural frequency of a finite conical bar

3.1 Clamped-clamped bar

For a clamped-clamped bar, the boundary conditions $u(0,t)=u(L,t)=0$ imply that $v(0,t)=v(L,t)=0$. Therefore, the natural frequencies of the conical bar are the same as those of a uniform bar and are given by

$$\omega_n = \frac{n\pi}{L}\sqrt{\frac{E}{\rho}} \tag{C.15}$$

In this case, the mode shapes are given by

$$\phi_n = \frac{1}{1+\alpha x/L}\sin k_{l,n}x \tag{C.16}$$

which indicates that, even though the natural frequencies are independent of the parameter α, the mode shapes are affected by it.

3.2 Free-clamped bar

For a free-clamped bar, the boundary conditions $\partial u(0,t)/\partial x = 0$ and $u(L,t)=0$ yield

$$\begin{aligned} -\frac{\alpha}{L}(C_1+C_2)+(-\mathrm{i}k_lC_1+\mathrm{i}k_lC_2)&=0 \\ \frac{1}{1+\alpha}\left(C_1e^{-\mathrm{i}k_lL}+C_2e^{+\mathrm{i}k_lL}\right)&=0 \end{aligned} \tag{C.17a, b}$$

From equation (C.17), the transcendental equation

$$\tan k_lL = -\frac{k_lL}{\alpha} \tag{C.18}$$

can be obtained. The case $\alpha=0$ gives the same result as a uniform bar, whose resonance occurs when k_lL is an odd multiple of $\pi/2$, namely

$$k_l L = \frac{(2n-1)\pi}{2} \tag{C.19}$$

Figure C-2 shows lines $y = \tan k_l L$ and $y = -k_l L/\alpha$. Natural frequencies can be determined by the intersections of $y = \tan k_l L$ and $y = -k_l L/\alpha$. It can be seen that the values of $k_l L$ at resonances of the gradually increasing conical bar ($\alpha = 1$) are higher than those of a uniform bar but the values of $k_l L$ at resonances of the gradually decreasing conical bar ($\alpha = -0.5$) are lower than those of a uniform bar. It can also be seen that the lowest mode is most affected by the particular value of α. However, the higher modes are less affected since, for higher modes, the line $y = -k_l L/\alpha$ intersects the line $y = \tan k_l L$ for a value of $k_l L$ very close to an odd multiple of $\pi/2$ [5].

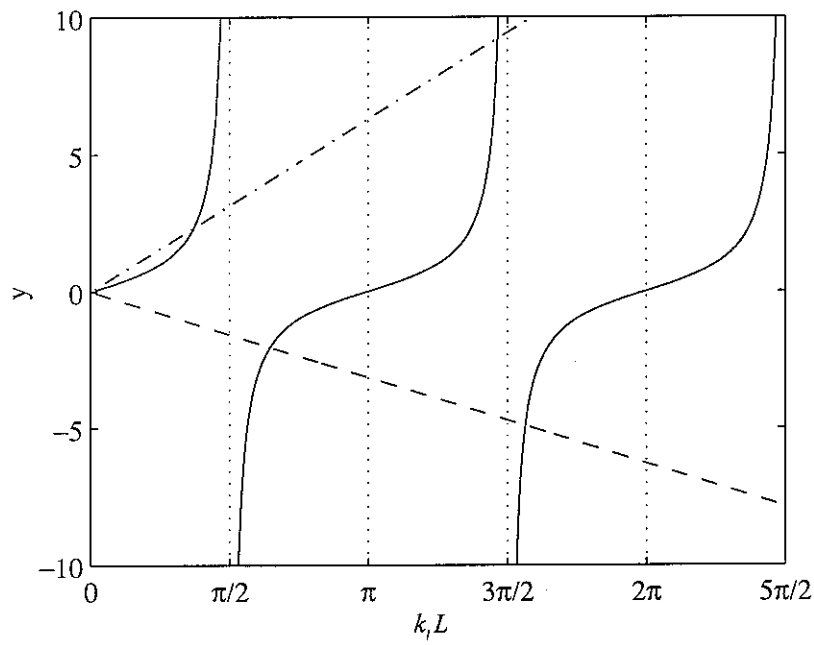

Figure C-2. Graphical determination of natural frequencies of conical bars.

——— , $y = \tan k_l L$; ------ , $y = -k_l L/\alpha$ for $\alpha = 1$; ·-·-·- , $y = -k_l L/\alpha$ for $\alpha = -0.5$.

References

1. A. D. Pierce 1981 *Acoustics: An Introduction to Its Physical Principles and Applications.* New York: McGraw-Hill.
2. H. D. Conway, E. C. H. Becker and J. F. Dubil 1964 *Transactions of the American Society Mechanical Engineers, Journal of Applied Mechanics* **31**, 329-331. Vibration frequencies of tapered bars and circular plates.
3. H. H. Mabie and C. B. Rogers 1968 *Journal of the Acoustical Society of America* **44**, 1739-1741. Transverse vibrations of tapered cantilever beams with end support.
4. H. H. Mabie and C. B. Rogers 1972 *Journal of the Acoustical Society of America* **55**, 986-991. Transverse vibrations of double-tapered cantilever beams with end support and with end mass.
5. S. Abrate 1995 *Journal of Sound and Vibration* **185**, 703-716. Vibration of non-uniform rods and beams.
6. B. M. Kumar and R. I. Sujith 1997 *Journal of Sound and Vibration* **207**, 721-729. Exact solutions for the longitudinal vibration of non-uniform rods.
7. L. Cremer, M. Heckl and E. E. Ungar 1973 *Structure-borne Sound.* Berlin:Springer-Verlag.
8. B. R. Mace 1984 *Journal of Sound and Vibration* **97**, 237-246. Wave reflection and transmission in beams.
9. Y. K. Lin and B. K. Donaldson 1969 *Journal of Sound and Vibration* **10**, 103-143. A brief survey of transfer matrix techniques with special reference to the analysis of aircraft panels.
10. D. H. Hodges, Y. Y. Chung and X. Y. Shang 1994 *Journal of Sound and Vibration* **169**, 276-

283. Discrete transfer matrix method for non-uniform rotating beams.

11. R. S. Langley 1995 *Journal of Sound and Vibration* **188**, 717-743. Wave transmission through one-dimensional near periodic structures: optimum and random disorder.
12. E. C. Pestel and F. A. Leckie 1963 *Matrix Methods in Elastomechanics*. New York: McGraw-Hill.
13. S. S. Rao 1995 *Mechanical Vibrations (3rd Edition)*. Reading, Mass.: Addison-Wesley.
14. N. R. Harland, B. R. Mace and R. W. Jones 2001 *Journal of Sound and Vibration* **241**, 735-754. Wave propagation, reflection and transmission in tunable fluid-filled beams.
15. R. G. White and J. G. Walker 1982 *Noise and Vibration Control*. Ellis Horwood Ltd.
16. L. Fox 1964 An Introduction to Numerical Linear Algebra. Oxford University Press.
17. D. J. Thompson and B. R. Mace 2003 *ISVR Lecture Course, Lecture notes on High Frequency Structural Vibration*. ISVR, Southampton.
18. D. W. Miller and A. Von Flotow 1989 *Journal of Sound and Vibration* **128**, 145-162. A travelling wave approach to power flow in structural networks.